



저작자표시-비영리-변경금지 2.0 대한민국

이용자는 아래의 조건을 따르는 경우에 한하여 자유롭게

- 이 저작물을 복제, 배포, 전송, 전시, 공연 및 방송할 수 있습니다.

다음과 같은 조건을 따라야 합니다:



저작자표시. 귀하는 원저작자를 표시하여야 합니다.



비영리. 귀하는 이 저작물을 영리 목적으로 이용할 수 없습니다.



변경금지. 귀하는 이 저작물을 개작, 변형 또는 가공할 수 없습니다.

- 귀하는, 이 저작물의 재이용이나 배포의 경우, 이 저작물에 적용된 이용허락조건을 명확하게 나타내어야 합니다.
- 저작권자로부터 별도의 허가를 받으면 이러한 조건들은 적용되지 않습니다.

저작권법에 따른 이용자의 권리는 위의 내용에 의하여 영향을 받지 않습니다.

이것은 [이용허락규약\(Legal Code\)](#)을 이해하기 쉽게 요약한 것입니다.

[Disclaimer](#)

The therapeutic role of
histone deacetylase (HDAC) inhibition
in an in vitro model of Graves' orbitopathy

Hyeong Ju Byeon

Department of Medicine

The Graduate School, Yonsei University

The therapeutic role of
histone deacetylase (HDAC) inhibition
in an in vitro model of Graves' orbitopathy

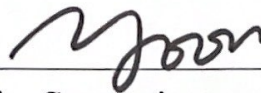
Directed by Professor Jin Sook Yoon

The Doctoral Dissertation
submitted to the Department of Medicine,
the Graduate School of Yonsei University
in partial fulfillment of the requirements for the degree of
Doctor of Philosophy in Medical Science

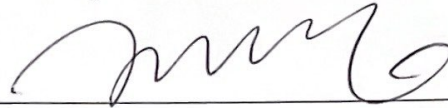
Hyeong Ju Byeon

December 2023

This certifies that the Doctoral Dissertation of
Hyeong Ju Byeon is approved.



Thesis Supervisor : Jin Sook Yoon



Thesis Committee Member#1 : Ja Seung Koo



Thesis Committee Member#2 : Eun Jig Lee



Thesis Committee Member#3: Joon H. Lee



Thesis Committee Member#4: Sang Wook Kang

The Graduate School
Yonsei University

December 2023

ACKNOWLEDGEMENTS

First and foremost, I'm deeply thankful to my thesis supervisor, Dr. Jin Sook Yoon. She has guided me both in my basic research and in clinical aspects. Her teachings have shaped my academic journey.

I also owe a big thank you to Dr. Ja Seung Koo. Even with his busy schedule, he took the time to help my thesis grow, offering clear directions and important feedback. I appreciate the guidance from Dr. Eun Jig Lee, Dr. Joon H. Lee, and Dr. Sang Wook Kang. They've shown me important areas in my research and gave suggestions on its future direction. I also am grateful to Dr. JaeSang Ko too. His advice and teachings, especially from a doctor's perspective, have been invaluable to me.

Lastly, I can't forget my family. They always stood by me. A special thank you to my parents-in-law for their support. And to my husband, Hyunwook Kim, who's been my rock, and to my lovely son, Dohoon, who always makes me smile, thank you.

<TABLE OF CONTENTS>

ABSTRACT	v
I. INTRODUCTION	1
II. MATERIALS AND METHODS	5
1. Reagents and chemicals	5
2. Tissue and cell preparation	5
3. Peripheral blood mononuclear cells (PBMC) preparation	7
4. Cell viability test	7
5. Real-time polymerase chain reaction (RT-PCR)	8
6. Western blot assays	9
7. Adipogenesis	9
8. Oil Red O staining	10
9. Silencing of HDAC	10
10. Statistical analysis	11
III. RESULTS	12
1. mRNA levels of HDACs in orbital tissue and PBMC	12
2. Effect of Panobinostat on cell viability	13
3. Suppression of HDACs by Panobinostat in GO orbital fibroblasts	14
4. Treatment effect of Panobinostat on stimulated orbital fibroblasts	15
5. The effect of Panobinostat on signaling pathway molecules	20
6. The role of HDAC7 in GO orbital fibroblasts	25
IV. DISCUSSION	33
V. CONCLUSION	38

REFERENCES	39
ABSTRACT(IN KOREAN)	44

LIST OF FIGURES

Figure 1. HDAC mRNA expression in GO and normal orbital tissues	12
Figure 2. HDAC mRNA expression level in PBMC	13
Figure 3. Cell viability after treatment with Panobinostat	14
Figure 4. Effect of Panobinostat on HDACs mRNA expression	15
Figure 5. Suppressive effect of Panobinostat on the expression of proinflammatory cytokines	16
Figure 6. Suppressive effect of Panobinostat on the expression of TGF- β -induced profibrotic proteins	17
Figure 7. Suppressive effect of Panobinostat on adipogenesis	19
Figure 8. Effect of Panobinostat on signal proteins under IL-1 β stimulation	21
Figure 9. Effect of Panobinostat on signal proteins under TGF- β stimulation	23
Figure 10. HDAC7 expression under stimulation of IL-1 β and TGF- β in GO orbital fibroblasts	26
Figure 11. Anti-inflammatory and anti-fibrotic effects of silencing HDAC7 in orbital fibroblasts	28
Figure 12. Effect of silencing HDAC6 on inflammation and fibrosis	30
Figure 13. Expression of HDAC3 and HDAC7 in Panobinostat treatment and HDAC7 siRNA transfection	31

LIST OF TABLES

Table 1. Clinical data of patients used in this study	6
Table 2. Demographics of subjects used for peripheral blood analysis	7
Table 3. Primers for quantitative PCR	8
Table 4. Small interfering RNA sequence	10

<ABSTRACT>

**The therapeutic role of histone deacetylase (HDAC) inhibition
in an in vitro model of Graves' orbitopathy**

Hyeong Ju Byeon

*Department of Medicine
The Graduate School, Yonsei University*

(Directed by Professor Jin Sook Yoon)

Graves' orbitopathy (GO) manifested by Graves' disease (GD) is characterized by orbital fibroblast-induced inflammation leading to fibrosis or adipogenesis. Histone deacetylases (HDACs) counteracting histone acetyltransferase activity play a central role in modifying autoimmune diseases and fibrosis. Moreover, HDAC inhibitors have been approved for use against hematologic malignancies. We investigated HDAC inhibition in orbital fibroblast from Graves' orbitopathy in order to evaluate its potential as a therapeutic agent. HDACs gene expression levels in orbital tissues and peripheral blood mononuclear cells (PBMC) were screened. The effect of the HDAC inhibitor, Panobinostat, on orbital fibroblasts was examined. Primary cultured orbital fibroblasts from GO and normal subjects were treated with Panobinostat under the stimulation of IL-1 β or TGF- β . Adipocyte differentiation was made in an adipogenic medium adding IL-1 β . Inflammatory cytokines, fibrosis, and adipogenesis-related proteins were analyzed using western blotting. To evaluate the selectivity of Panobinostat, the effect of Panobinostat on the expression of HDACs mRNA was measured in GO orbital fibroblasts using real-time PCR and HDAC7 was knocked down using small interfering RNA (siRNA) transfection. Using Oil Red O, cells were stained to quantify lipid accumulation. Panobinostat reduced the production of IL-1 β -induced inflammatory cytokines such as IL-6, IL-8, and TGF- β -induced fibrosis-related proteins such as collagen I α 3, α -SMA, and fibronectin. In addition, Panobinostat

suppressed adipocyte differentiation and production of C/EBP α / β , aP2, adiponectin, leptin, and PPAR γ proteins. Panobinostat significantly attenuated HDAC7 mRNA expression in orbital fibroblasts from GO, and the silencing of HDAC7 also showed anti-inflammatory and anti-fibrotic effects. Panobinostat by inhibiting HDAC7 gene expression, suppressed the production of inflammatory cytokines, profibrotic proteins, and adipogenesis in GO orbital fibroblasts. Our in vitro study using primary cultured orbital fibroblasts suggests that HDAC7 can be a potential therapeutic target to inhibit inflammation, adipogenesis, and fibrotic mechanisms of GO.

Key words : Graves orbitopathy, orbital fibroblasts, HDAC inhibitor, Panobinostat, HDAC7,

The therapeutic role of histone deacetylase (HDAC) inhibition in an in vitro model of Graves' orbitopathy

Hyeong Ju Byeon

*Department of Medicine
The Graduate School, Yonsei University*

(Directed by Professor Jin Sook Yoon)

I. INTRODUCTION

Graves' ophthalmopathy (GO) is an orbital inflammation in approximately 15% to 30% of Graves' disease (GD).^{1,2} GO has a presentation of eyelid retraction, exophthalmos, and extraocular muscle enlargement; 3-5% have experienced vision-threatening severe form including compressive optic neuropathy and corneal exposure.^{2,3}

Dysregulated orbital fibroblasts and orchestrated mononuclear cells play a key role in the pathogenesis of GO. Autoantibodies to thyrotropin receptor and insulin-like growth factor 1 receptor (IGF-1R) activate infiltration of mononuclear cells such as T cells, B cells, and macrophages.⁴ Mononuclear cells that have been activated, particularly CD4⁺ T cells, release cytokines that stimulate orbital fibroblast and moreover, orbital fibroblast itself produces proinflammatory cytokines that exacerbate and maintain ocular inflammation.^{2,5} Stimulated orbital fibroblasts proliferate to produce glycosaminoglycans (GAG) and differentiate into adipocytes or myofibroblasts, which eventually leads to orbital tissue swelling, enlargement, and fibrosis.

First-line treatment in GO is glucocorticoid to alleviate inflammation induced by autoimmunity but has systemic complications. Teprotumumab, recently approved by the United States Food and Drug Administration (US FDA), is IGF-1R monoclonal antibody that intervenes the initiation of inflammation but it is so far defined to the patients who

have high clinical activity score (CAS) and has limitations in about one-third of responders show relapse during the year after cessation.^{6,7} It also carries critical adverse effects including hearing loss, hyperglycemia, and muscle spasm. The ultimate goal is to cut the immune reaction occurring around the orbital fibroblast. Therefore, gaining a deeper knowledge of the molecular mechanisms underlying the pathophysiology of GO could lead to the discovery of new therapeutic targets.

As a part of the effort approaching the pathogenesis and finding treatment of GO, genetic susceptibility emerged in the past decade, however, there was no significant evidence of genotypic or allele differences between GO and non-GO patients.^{8,9} Nowadays, the research focuses on the epigenetic and/or environmental factors; gut microbiome, DNA methylation, miRNA, and histone modification.¹⁰

Histone deacetylase (HDAC), counteract of histone acetyltransferase (HAT), is one of the promising molecules in epigenetics. Based on their enzymatic domain organization, the eighteen HDACs are classified into four groups, and Zn²⁺ dependent HDACs are called classical HDACs; Class I (HDAC 1,2,3,8), Class II a (HDAC 4,5,7,9), Class II b (HDAC 6,10), and Class IV (HDAC 11), whereas Class III (Sirtuins) is mediated through NAD⁺ dependently. HDACs mediate the deacetylation of lysine residues on the histone tail as post-translational modification and make DNA tighten around the nucleosome, consequently inhibiting transcription factor access to DNA.¹¹ This modification regulates gene transcription controlling the cell cycle or immunologic pathway.¹² Moreover, in addition to histone protein, lysine acetylation occurs in several non-histone proteins, including transcription factors or proteins involved in metabolism and cell cycle.¹³ HDAC inhibitors (HDACis) have been approved for hematologic anti-tumor activity by inhibiting various pathways involving cytokines, growth factors, and protein kinases,¹⁴ however, the role of HDAC and related cytokines needs to be elucidated in autoimmune diseases.

Similar to orbital fibroblast, lung fibroblast and synovial fibroblast have been appreciated as active participants in autoimmune diseases.¹⁵ The role of HDAC has been researched a

lot in the lungs and synovium. In rheumatoid arthritis (RA), the first FDA-approved pan-HDACi, Vorinostat, when treated with synovial fibroblast, induced apoptosis and reduced NF- κ B phosphorylation and anti-apoptotic proteins (Bcl-xL and Mcl-1) expression.¹⁶ Trichostatin A, another pan-HDACi, lowered synovial fibroblast viability and reduced the expression of matrix metalloproteinases (MMP)-2, MMP-9, with inactivation of PI3K/Akt pathway.¹⁷ HDAC6 specific inhibitor decreased the arthritis score in the collagen-induced arthritis model and reduced the expression of TNF- α and IL-1 β in RA patients.¹⁸ Also, the inhibition of HDAC6 was reported to enhance the suppressive activity of regulatory T cells in inflammation and autoimmunity.^{18,19}

HDACs in the lung have been researched focused on pulmonary fibrosis, which has pathogenesis of the apoptosis-resistant cell character producing extracellular matrix persistently. With human primary idiopathic pulmonary fibrosis (IPF) lung fibroblasts, TGF- β mediated anti-fibrotic gene repression promoted fibroblast activation and HDAC7 was a key factor in fibrosis.²⁰ IPF-fibroblast treated with pan-HDACi, Panobinostat, show decreased phosphorylated STAT3 protein level and survival-related gene Bcl-XL and BIRC5/surviving expression.²¹ Similar results also have been reported as Vorinostat induce apoptosis and lung function was improved in the murine model.²²

The role of HDAC in GO pathogenesis needs to be broadly explored. Among the HDAC is that have been approved to exhibit hematologic anti-tumor activity, Panobinostat (LBH589), an orally available pan-HDACi, was approved by US FDA in 2015 as a drug for the treatment of multiple myeloma.¹⁴ Panobinostat had at least ten-fold more potency of anti-cancer effect compared to Vorinostat, and IC₅₀ (concentration needed for 50% inhibition) values were lower than the other pan-HDACis.^{23,24} In addition, Panobinostat showed superior anti-fibrotic effects in primary idiopathic pulmonary fibroblasts compared with Pirfenidone, the only currently covered IPF treatment.²¹

In this study, initial experiments evaluated the effects of pan-HDACi, Panobinostat, on GO pathogenesis by RT-PCR and western blot; inflammation, adipogenesis, and fibrosis. Additional experiments were performed to assess which HDAC exerts the therapeutic effect

of Panobinostat, and consequently, we focused on HDAC7. Finally, we could conclude that Panobinostat showed anti-inflammatory, anti-fibrotic, and anti-adipogenic effects through HDAC7 regulation in GO fibroblasts, therefore, HDAC7 could be a potential target for GO treatment.

II. MATERIALS AND METHODS

1. Reagents and chemicals

The following reagents were used in the study: Dulbecco's modified Eagle's medium/Nutrient Mixture F-12 (DMEM/F12, 1:1); penicillin/streptomycin (Welgene, Gyeongsan-si, Gyeongsangbuk-do, South Korea); fetal bovine serum (FBS) (Gibco; Thermo Fisher Scientific, Waltham, MA, USA); Panobinostat (Selleckchem, Huston, TX, USA); recombinant IL-1 β and TGF- β (R&D Systems, Minneapolis, UT, USA); antibodies for IL-6, IL-8, HDAC6, HDAC7, CCAAT/enhancer-binding protein (C/EBP) α , phosphorylated (p)-Akt, total (t)-Akt, p-extracellular signal-related kinase (ERK), t-ERK, p-p38, t-p38, p-c-Jun N-terminal kinases (JNK), t-JNK, p-nuclear factor (NF) κ B, t-NF κ B, p-SMAD1/5/9, t-SMAD1/5/9, p-SMAD2, t-SMAD2, p-SMAD3, t-SMAD3 in western blot (Cell Signalling Technology, Danvers, MA, USA); Fibronectin antibody (BD, Franklin Lakes, NJ, USA); Collagen I α antibody (Abcam, Cambridge, UK); α -smooth muscle actin (SMA) antibody (Sigma-Aldrich, St. Louis, MO, USA); anti-Collagen 3, HDAC3, C/EBP β , adiponectin, leptin(ob), adipocyte protein 2 (aP2), peroxisome proliferator-activated receptor (PPAR) γ , β -actin antibodies (Santa Cruz Biotechnology, Santa Cruz, CA, USA).

2. Tissue and cell preparation

Orbital adipose tissues were obtained during surgeries. GO tissues were collected from orbital decompression surgery in 10 patients (4 men and 6 women, age 22-65). All patients at the time of surgery had achieved euthyroid status and a CAS less than 3. For the control group, normal tissues were harvested in 8 patients (4 men and 4 women, age 37-75) during upper or lower eyelid blepharoplasty and orbital fat prolapse, who had not been diagnosed as GO or autoimmune thyroid disease (Table 1). This study was approved by the institutional review board of Severance Hospital, Yonsei University College of Medicine (Seoul, Korea) (IRB number: 4-2022-0244) and all the subjects provided written informed consent. This study abides by the tenets of the Declaration of Helsinki.

Table 1. Clinical data of patients used in this study.

Age (years)	Sex	CAS	Duration of GO (years)	Proptosis R/L (mm)	Surgery performed
GO patients					
57	F	0	1	17/16	Orbital decompression
22	F	1	5	21/22	Orbital decompression
45	M	1	1	16/15	Orbital decompression
48	F	0	13	20/20	Orbital decompression
27	F	2	2	20/23	Orbital decompression
23	M	0	3	21/20	Orbital decompression
63	M	1	7	20/24	Orbital decompression
65	F	0	2	23/23	Orbital decompression
25	F	0	3	20.5/21	Orbital decompression
36	M	0	3	25/26	Orbital decompression
Normal control subjects					
75	F	n/a	n/a	n/a	Upper lid blepharoplasty
74	M	n/a	n/a	n/a	Lower lid blepharoplasty
68	M	n/a	n/a	n/a	Upper lid blepharoplasty
76	F	n/a	n/a	n/a	Upper lid blepharoplasty
56	M	n/a	n/a	n/a	Orbital fat prolapse removal
37	F	n/a	n/a	n/a	Upper lid blepharoplasty
61	M	n/a	n/a	n/a	Upper lid blepharoplasty
61	F	n/a	n/a	n/a	Lower lid blepharoplasty

GO, Graves' orbitopathy; CAS, clinical activity scores; n/a; not applicable; F, female; M, male; R, right eye; L, left eye.

Orbital fat tissues to be used for RNA preparation were collected in RNAlater (Invitrogen, Carlsbad, CA, USA) for long-term storage. For primary cell culture, orbital fat tissues were minced and distributed in DMEM/F12 containing 20% FBS, 1% penicillin/streptomycin. As orbital fibroblasts proliferated, the cells were passaged serially with trypsin/ethylenediaminetetraacetic acid (EDTA) and incubated with DMEM:F12 containing 10% FBS and 1% penicillin/streptomycin. Strains under the 4th passage were stored in liquid nitrogen for subsequent use. The orbital fibroblasts were grown to confluence in 10 cm dishes in a humidified 5% CO₂ incubator at 37°C. The cultured cells were plated in 6-well plates, and the culture medium was changed to serum-free

DMEM/F12 containing 1% penicillin/streptomycin before reagent treatment.

3. Peripheral blood mononuclear cells (PBMC) preparation

A total of 10ml peripheral venous blood from healthy donors and GO patients was used for PBMC isolation by Ficoll-Paque (Cytiva, Marlborough, MA, USA) density-gradient centrifugation (Table 2). For long-term storage, isolated PBMCs were preserved in TriZol (Invitrogen) reagent at a -80°C freezer. Extracted RNA from PBMC was used for real-time polymerase chain reaction.

Table 2. Demographics of subjects used for peripheral blood analysis.

	Normal control (N=11)	GO patients (N=32)	<i>p-value</i>
Age, years (range)	44.5 ± 16.9 (21-83)	40.2 ± 13.0 (18-76)	0.68
Sex (M : F)	3 : 8	13 : 19	0.67
Graves' disease duration, years	-	5.5 ± 4.3	-
GO CAS (range)	-	1.5 ± 1.7 (0-5)	-
Thyroid lab (normal range)			
T3 (ng/mL) (0.61-1.16)	-	1.1 ± 0.5	-
Free T4 (ng/mL) (0.80-1.23)	-	1.0 ± 0.4	-
TSH ($\mu\text{IU/mL}$) (0.41-4.30)	-	1.9 ± 2.7	-
TRAb (IU/L) (0-1.75)	-	11.4 ± 12.1	-
TSI (SRR,%) (0-140%, negative)	-	251.7 ± 131.7	-

GO, Graves orbitopathy; TSH, Thyroid stimulating hormone; TSI, Thyroid stimulating immunoglobulin; TRAb, Thyroid stimulating hormone receptor antibody; SRR, specimen-to-reference ratio.

Data are represented as mean ± standard deviation or number.

4. Cell viability test

Orbital fibroblasts from GO patients and normal subjects were seeded into 24-well culture plates at a density of 1×10^5 cells/well and exposed to various concentrations of Panobinostat (control, 10, 30, 50, 70, and 100 nM) for 24 hours in order to determine the non-cytotoxic concentration for these cells. Following exposure, cells were cleaned and incubated with a 5 mg/mL MTT solution (3-[4,5-dimethylthiazol-2-yl]-2,5-

diphenyltetrazolium bromide; Sigma Aldrich) for 2 hours at 37 °C. A microplate reader (EL 340 Bio Kinetics Reader; Bio-Teck Instruments, Winooski, VT, USA) was used to measure the dye's absorbance at 560 nm and 630nm after it had been solubilized with DMSO (dimethyl sulfoxide; Sigma-Aldrich). In comparison to untreated control cells, cell viability was expressed as a percentage.

5. Real-time polymerase chain reaction (RT-PCR)

A tissue homogenizer (Precellys 24; Bertin Instruments, Montigny-le-Bretonneux, France) was used to homogenize the harvested orbital fat tissues, and tissues were lysed with a Precelly lysing kit (Bertin Instruments) with TriZol. Primary cultured GO orbital fibroblasts treated with Panobinostat were also lysed with TriZol. The RNA concentration was determined using NanoDrop (Thermo Fisher Scientific, Waltham, MA, USA). cDNA was synthesized according to the manufacturer's protocol (SensiFAST cDNA Synthesis Kit; Meridian Life Science, Inc., Memphis, TN, USA). PCR amplification was performed using QuantStudio3 real-time PCR thermocycler (Applied Biosystems, Carlsbad, CA, USA) with specific primers and SYBR green PCR master mix (Takara Bio, Inc., Shiga, Japan). Primer sequences specific for multiple *HDACs* (class I *HDACs*; *HDAC1, 2, 3*, class IIa *HDACs*; *HDAC4, 5, 7*, class IIb *HDACs*; *HDAC6, 10*) are described in Table 3. The results were normalized against glyceraldehyde-3-phosphate dehydrogenase (GAPDH) and presented as the fold change in cycle threshold (Ct) value relative to the control group, calculated using the $2^{-\Delta\Delta Ct}$ method.

Table 3. Primers for quantitative PCR

Name	Primer sequences (5'-3')	
HDAC1	Forward	CTA CTA CGA CGG GGA TGT TGG
	Reverse	GAG TCA TGC GGA TTC GGT GAG
HDAC2	Forward	ATG GCG TAC AGT CAA GGA GG
	Reverse	TGC GGA TTC TAT GAG GCT TCA
HDAC3	Forward	CCT GGC ATT GAC CCA TAG CC
	Reverse	CTC TTG GTG AAG CCT TGC ATA

HDAC4	Forward	GGC CCA CCG GAA TCT GAA
	Reverse	GAA CTC TGG TCA AGG GAA CTG
HDAC5	Forward	TCT TGT CGA AGT CAA AGG AGC
	Reverse	GAG GGG AAC TCT GGT CCA AAG
HDAC6	Forward	AGC GGA GGT AAA GAA GAA AGG CAA AAT G
	Reverse	CCA GGC AGG CAC AGG AGT ATG AGT T
HDAC7	Forward	GGC GGC CCT AGA AAG AAC AG
	Reverse	CTT GGG CTT ATA GCG CAG CTT
HDAC10	Forward	TGG CAC CGC TAT GAG CAT
	Reverse	GAG ACC AGC ACC AGC TCA G
GAPDH	Forward	ATG GGG AAG GTG AAG GTC G
	Reverse	GGG GTC ATT GAT GGC AAC AAT A

6. Western blot

Orbital fibroblasts treated with a reagent in accordance with the study plan were washed with Dulbecco's phosphate-buffered saline solution (Welgene) and then lysed using RIPA lysis buffer (Welgene) containing a Halt™ Protease Inhibitor Cocktail (#1860932 Thermo Fisher Scientific). After being resolved in 8-15% SDS-PAGE, the cell lysates were transferred to nitrocellulose membranes (Millipore Corp., Billerica, MA, USA). After that, primary antibodies were applied to the membranes for a whole night at 4°C. Using an image reader (LAS-4000 mini; Fuji Photo Film, Tokyo, Japan), immunoreactive bands were identified using a secondary antibody coupled to horseradish peroxidase with a chemiluminescent substrate (Thermo Fisher Scientific). To quantify the protein level, the intensities of the band were measured using Image J software (National Institutes of Health, Bethesda, Maryland, USA) as a densitometry analysis and standardized to those of the β -actin in the same sample.

7. Adipogenesis

Orbital fibroblasts were differentiated into adipocytes for 14 days. During the fourteen days, cells grown in 6-well plates were stimulated with adipogenic solutions; DMEM high glucose (Welgene) with 10% FBS and antibiotics, 33 μ M biotin (Sigma-Aldrich), 17 μ M pantothenic acid (Sigma-Aldrich), 10 μ g/mL transferrin (Sigma-aldrich), 0.2 nM T3

(Sigma-Aldrich), 1 μ M insulin (Boehringer-Mannheim, Mannheim, Germany), 0.2 μ M carbaprostaglandin (cPGI₂; Calbiochem, La Jolla, CA, USA) and 10 μ M rosiglitazone (Cayman, Ann Arbor, MI, USA). The media was replaced every 2-3 days. For the first 4 days, 10 μ M dexamethasone (Sigma-Aldrich) and 0.1 mM isobutylmethylxanthine (IBMX; Sigma-Aldrich) were also added. To assess the effect of Panobinostat on adipogenesis, cells were co-treated with Panobinostat (10nM) or IL-1 β (10ng/ml) for 14 days.

8. Oil Red O staining

To assess adipocyte differentiation, orbital fibroblasts were stained with Oil Red O. Cells were washed twice with 1 x PBS, fixed with 10% formalin in PBS for 1 hour at 4°C, then stained for 2 hours with 200 μ L Oil Red O (#O1516, Sigma-Aldrich) working solution (Oil Red O:DW=6:4, filtered). The plates were rinsed with PBS and observed using a microscope (IX73; Olympus Optical, Tokyo, Japan) with a charge-coupled device camera (DP71; Olympus Optical). To quantify lipid accumulation, Oil red O stain was solubilized with 100% isopropanol, and the optical density of the solution was determined using a spectrophotometer at 490nm.

9. Silencing of HDAC

Small interfering RNA (siRNA) designed to silence *HDAC6*, *HDAC7* genes were obtained from Dharmacon (Horizon Discovery, Cambridge, UK), and Silencer™ Select Negative Control No. 1 siRNA was from Invitrogen (Table 4). 10nM siRNAs were transfected into 80% confluent orbital fibroblasts with Lipofectamine RNAiMAX (Invitrogen) according to supplier instructions. The medium was changed to a fresh complete medium containing 10% FBS and antibiotics after 24 hours of transfection. Cells were maintained for 48 hours.

Table 4. Small interfering RNA sequence

Name	Sequences (5'-3')
Negative control	(Sense) UUC UCC GAA CGU GUC ACG UTT
	(Antisense) ACG UGA CAC GUU CGG AGA ATT
HDAC6	GGGAGGUUCUUGUGAGAUC
	GGAGGGUCCUUAUCGUAGA
	GCAGUUAAAUGAAUCCAU
	GUUCACAGCCUAGAAUAUA
HDAC7	GACAAGAGCAAGCGAAGUG
	GCAGAUACCCUCGGCUGAA
	GGUGAGGGCUUCA AUGUCA
	UGGCUGCUCUUCUGGGUAA

10. Statistical analysis

For statistical analysis, IBM SPSS Statistics for Windows v 29.0 (IBM Corp., Armonk, NY, USA) was used. All experiments were performed twice in cells from three different patients. The results were averaged and expressed as the mean values \pm standard deviation (SD). Normal distribution was verified with Kolmogorov–Smirnov test, and with the results, Student t-test or Mann–Whitney U-test was used to compare the differences between groups. A *p*-value less than 0.05 was considered statistically significant.

III. RESULTS

1. mRNA levels of HDACs in orbital tissue and PBMC

The basal levels of HDACs' transcript were analyzed by RT-PCR. Eight HDACs which included class I (HDAC 1,2,3), class IIa (HDAC 4,5,7), and class IIb (HDAC 6,10) were studied. In orbital tissues taken from GO subjects (n=10) and normal controls (n=8), median mRNA expression levels of *HDAC 3*, *4*, *5*, *6*, and *7* were significantly lower in GO patients (median mRNA relative expression level 0.493, 0.526, 0.552, 0.610, and 0.456 respectively, $*p < 0.05$) (Figure 1). We also investigated *HDAC* gene expression patterns in PBMC of GO patients (n=32) and normal controls (n=11). There were no significant differences in the mRNA expression of *HDACs* between GO and normal PBMC (Figure 2).

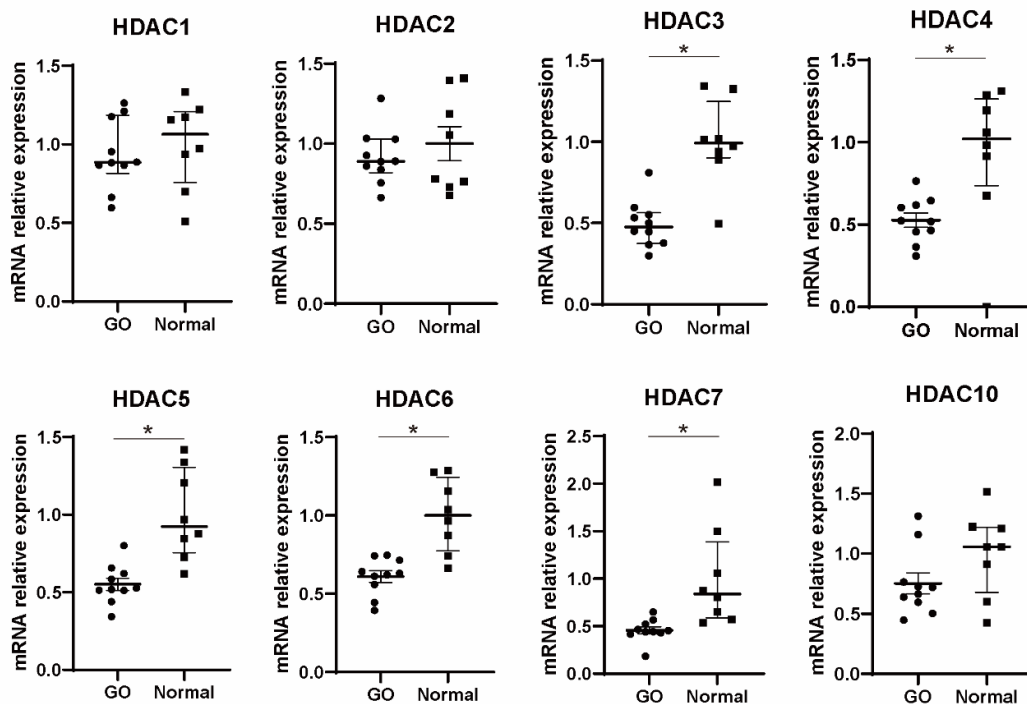


Figure 1. HDAC mRNA expression in GO and normal orbital tissues. Orbital tissues from GO (n=10) and normal subjects (n=8) were analyzed to evaluate the mRNA expression level of *HDACs* (class I HDACs; *HDAC1*, *2*, *3*, class IIa HDACs; *HDAC4*, *5*, *7*, class IIb

HDACs; *HDAC6, 10*). RT-PCR was performed, and the results are presented as the median and interquartile ranges ($*p < 0.05$ versus normal control).

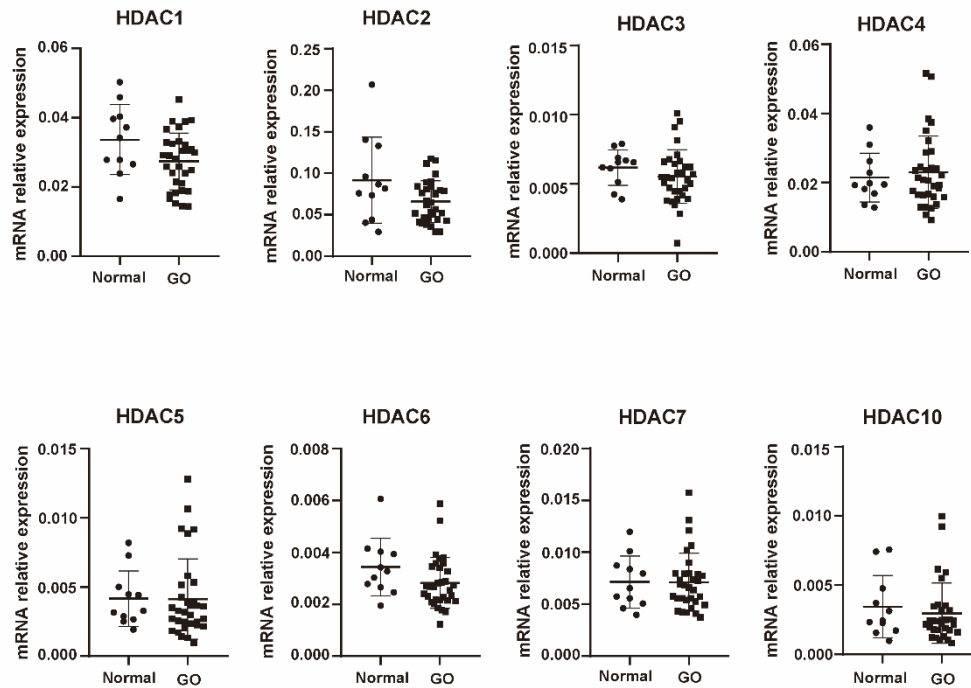


Figure 2. HDAC mRNA expression level in PBMC. PBMCs from GO patients (n=32) and normal control (n=11) were used. HDACs (class I HDACs; *HDAC1, 2, 3*, class IIa HDACs; *HDAC4, 5, 7*, class IIb HDACs; *HDAC6, 10*) mRNA expressions were determined by RT-PCR. The results are represented as median and interquartile ranges.

2. Effect of Panobinostat on cell viability

To assess the treatment effect of HDAC inhibition, a pan-HDACi, Panobinostat, was used. MTT assay was performed to determine the non-toxic concentration of Panobinostat. In both normal and GO orbital fibroblasts, Panobinostat at concentrations between 10 and 100nM did not reduce cell viability below 95% over the course of a 24-hour treatment (Figure 3).

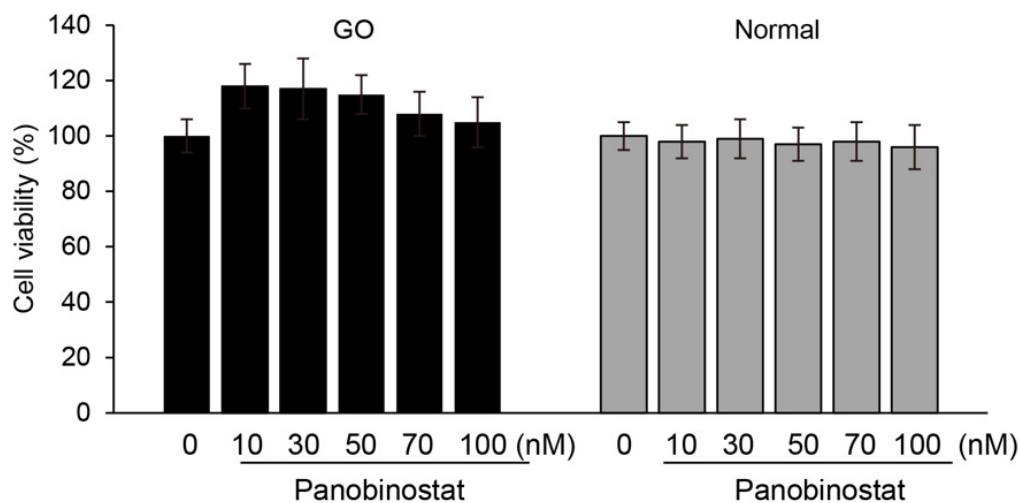


Figure 3. Cell viability after treatment with Panobinostat. Orbital fibroblasts from GO patients (n=3) and normal subjects (n=3) were seeded into 24-well culture plates and various concentrations of Panobinostat (control, 10, 30, 50, 70, and 100 nM) were treated for 24 hours. The MTT assays were repeated twice on three different individual cells. Results are represented as means \pm SD relative to untreated control.

3. Suppression of HDACs by Panobinostat in GO orbital fibroblasts

Even with Panobinostat which is known as a nonselective HDACi, not all HDACs are inhibited uniformly. Pan-HDACis could have different effects on each HDACs depending on the cell context.²⁵ To verify the selectivity of Panobinostat on GO orbital fibroblasts, GO orbital fibroblasts were incubated for 24 hours with and without Panobinostat (100nM), and the level of various *HDACs* transcripts were analyzed using RT-PCR; class I HDACs; *HDAC1, 2, 3*, class IIa HDACs; *HDAC4, 5, 7*, class IIb HDACs; *HDAC6, 10*. HDAC3 mRNA was upregulated and HDAC6 and HDAC7 mRNA were downregulated significantly ($*p < 0.05$) (Figure 4).

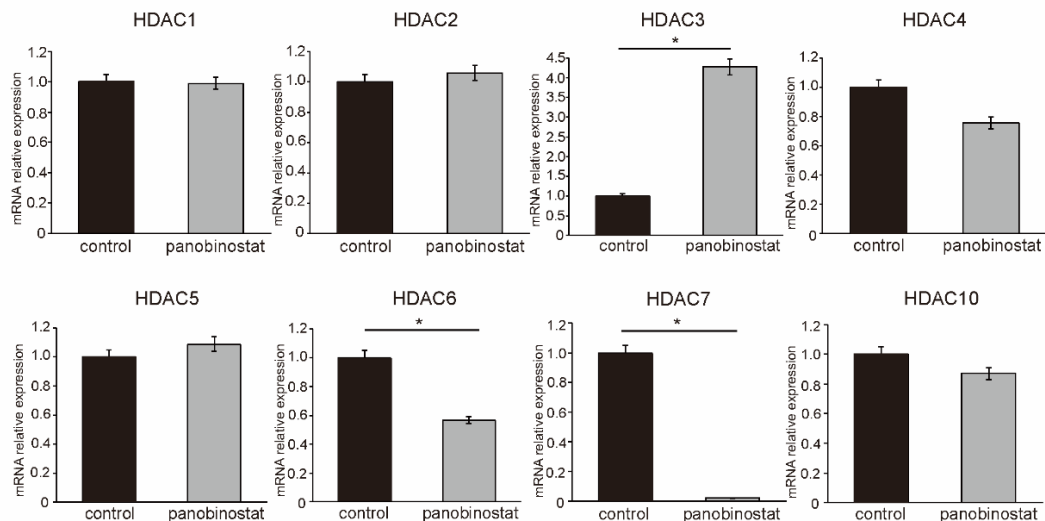


Figure 4. Effect of Panobinostat on HDACs mRNA expression. Orbital fibroblasts from GO (n=3) were cultured with Panobinostat (100 nM) for 24 hours. GO Orbital fibroblasts cultured without Panobinostat for 24 hours were compared as control. HDACs (class I HDACs; *HDAC1, 2, 3*, class IIa HDACs; *HDAC4, 5, 7*, class IIb HDACs; *HDAC6, 10*) mRNA expressions were measured by RT-PCR. All experiments were conducted twice in three different subjects and the graphs show mean \pm SD (* $p < 0.05$ versus control).

4. Treatment effect of Panobinostat on stimulated orbital fibroblasts

We evaluated the therapeutic effect of Panobinostat in multiple pathogenic processes of GO (inflammation, adipogenesis, and fibrosis) in primary cultured orbital fibroblasts. First, GO and normal orbital fibroblasts were pretreated with Panobinostat (100nM) for 30 minutes and inflammatory stimulation by IL-1 β (10ng/ml) was applied to the orbital fibroblasts for 24 hours. Western blot results showed that IL-1 β -induced proinflammatory cytokines, IL-6 and IL-8, were suppressed by the Panobinostat treatment (* $p < 0.05$) (Figure 5).

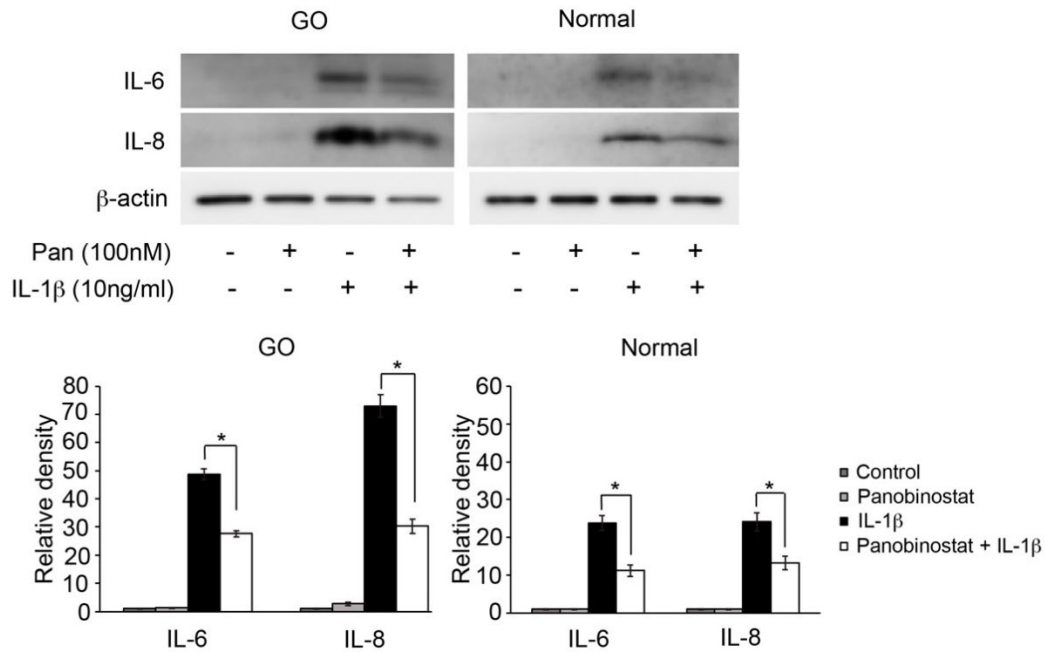


Figure 5. Suppressive effect of Panobinostat on the expression of proinflammatory cytokines. Orbital fibroblasts from GO (n=3) and normal subjects (n=3) were pretreated with Panobinostat (100nM) for 30 minutes and then stimulated with IL-1 β (10ng/ml) for 24 hours. Western blot was performed to measure the protein expression of proinflammatory cytokines, IL-6 and IL-8. Representative western blot gel images are shown. Western blot analysis was quantified with densitometry and normalized with β -actin in the same sample. Data in columns are represented as mean \pm SD of three independent experiments conducted in duplicate ($*p < 0.05$).

Second, in the same experimental condition, pretreatment stimulation was changed to TGF- β (5ng/ml) to investigate the anti-fibrotic effect. Increased protein expressions of profibrotic cytokines, fibronectin, collagen I α , and collagen 3, induced by TGF- β were significantly ameliorated after the treatment of Panobinostat ($*p < 0.05$) (Fig. 6).

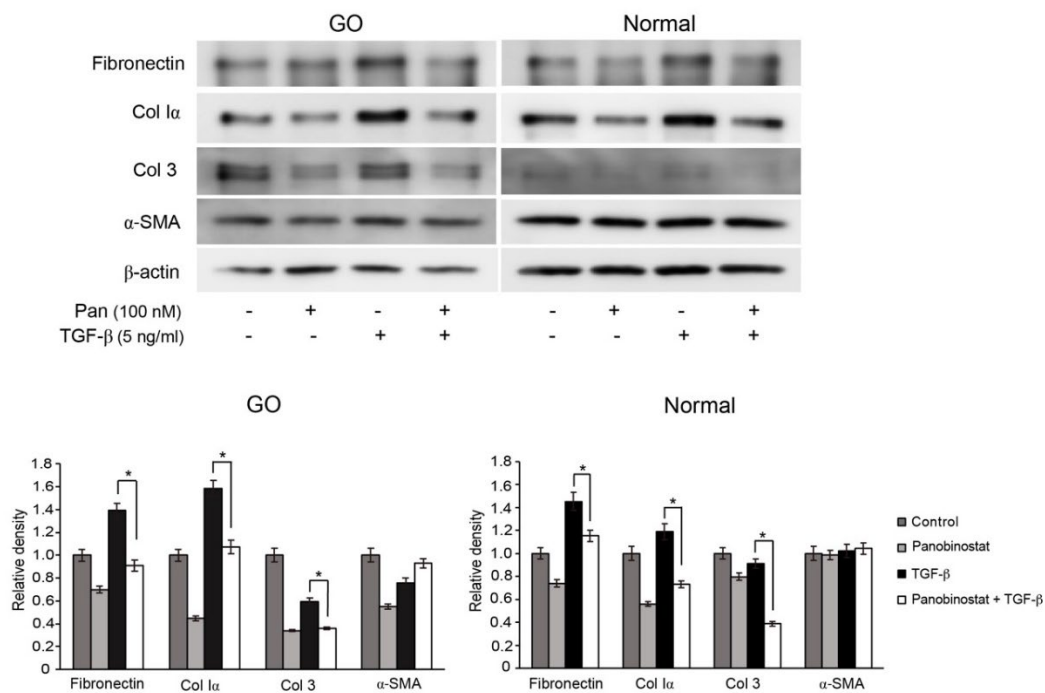


Figure 6. Suppressive effect of Panobinostat on the expression of TGF- β -induced profibrotic proteins. Orbital fibroblasts from GO (n=3) and normal controls (n=3) were pretreated with Panobinostat (100nM) for 30 minutes, followed by stimulation with TGF- β (5ng/ml) for 24 hours. Profibrotic proteins, fibronectin, collagen I α , collagen 3, and α -SMA, expression levels were determined by western blot analysis. Representative western blot gel images are shown. β -actin was used as a normalization for western blot analysis. Results represent mean \pm SD of three different individuals conducted in duplicate (* p <0.05).

Lastly, the Panobinostat effect on the adipocyte differentiation of orbital fibroblasts was examined. During the 14 days of adipogenesis cultured in an adipogenic medium, GO orbital fibroblasts were also co-treated with Panobinostat (10nM) or IL-1 β (10ng/ml). Panobinostat significantly attenuated IL-1 β induced adipogenesis (Figure 7A), as shown

by the lipid quantification under spectrophotometer at 490nm ($*p < 0.05$) (Figure 7B). Protein expression level of all the investigated adipogenic transcription factors, PPAR γ , C/EBP α , C/EBP β , aP2, adiponectin, and leptin(ob), and HDAC7 was reduced with the Panobinostat treatment ($*p < 0.05$) (Figure 7C, 7D).

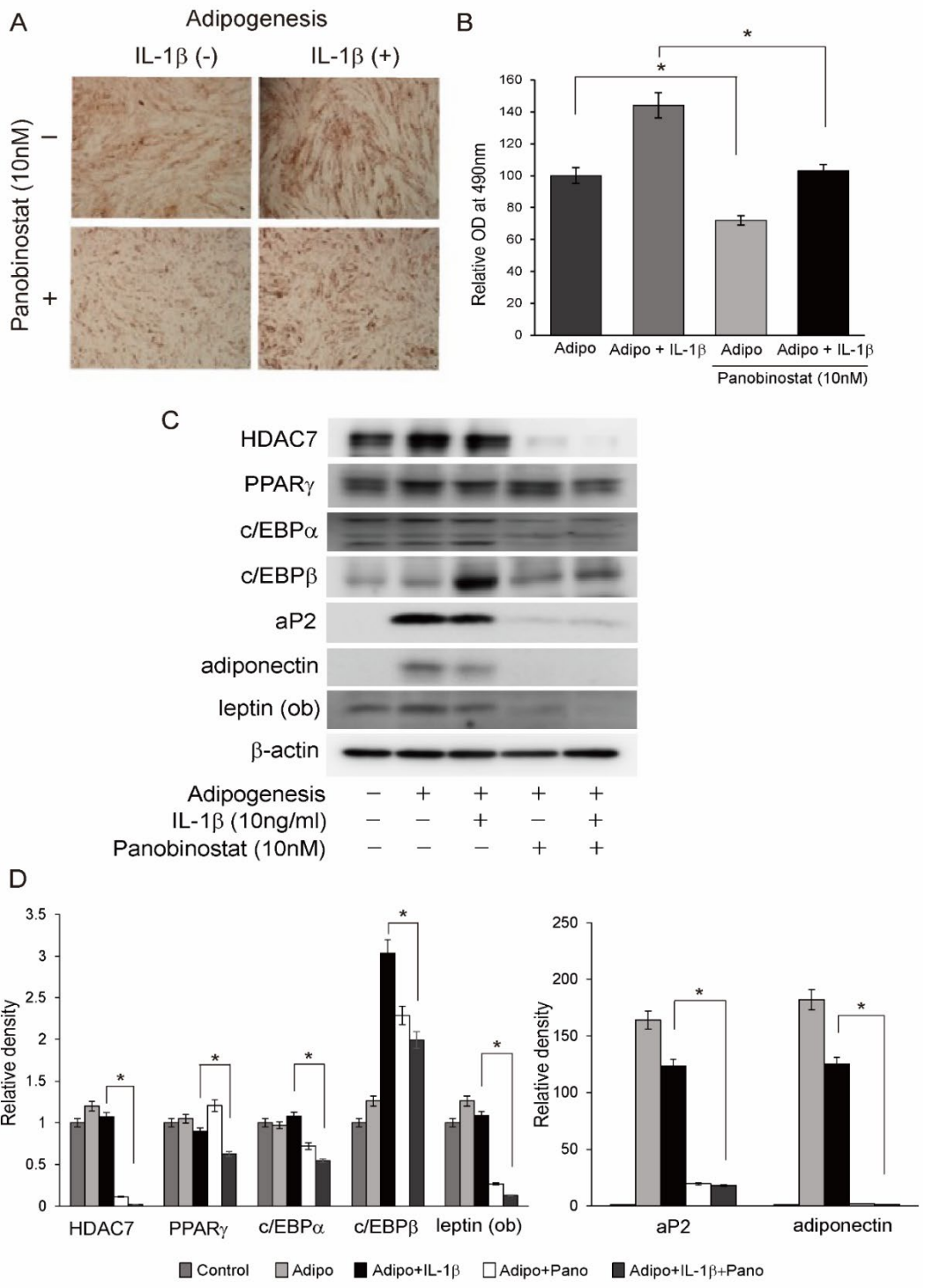


Figure 7. Suppressive effect of Panobinostat on adipogenesis. GO orbital fibroblasts (n=3) were differentiated into adipocytes under 14 days of incubation with adipogenic medium. Panobinostat (10nM) or IL-1 β (10ng/ml) was added during the adipogenesis of 14 days. All the experiments were performed twice. (A) To evaluate adipocyte differentiation, cells were stained with Oil Red O, and cytoplasmic lipid droplets were examined under microscopy (x 40). (B) Stained cell lysates were solubilized and measured with a spectrophotometer at 490nm. The graphs were represented as relative density with mean \pm SD (* p <0.05 versus without Panobinostat). (C) Adipogenic transcription factors, PPAR γ , C/EBP α , C/EBP β , aP2, adiponectin, leptin(ob), and HDAC7 were analyzed with western blotting after 14 days of adipogenic differentiation of orbital fibroblasts. Representative western blot gel images are shown. (D) Densitometer results of the western blot are shown as relative mean density \pm SD normalized to the β -actin (* p <0.05 versus without Panobinostat).

5. The effect of Panobinostat on signaling pathway molecules

After examining Panobinostat showed anti-inflammatory and anti-fibrotic effects, we further researched intracellular signaling pathway molecules with Panobinostat treatment. Orbital fibroblasts pretreated with Panobinostat (100nM) for 24 hours were incubated with IL-1 β (10ng/ml) for 15 minutes. Among the signaling pathway molecules, NF- κ B, Akt, JNK, and ERK, IL-1 β induced JNK and Akt phosphorylation were ameliorated with Panobinostat treatment in GO orbital fibroblasts (* p <0.05) (Figure 8).

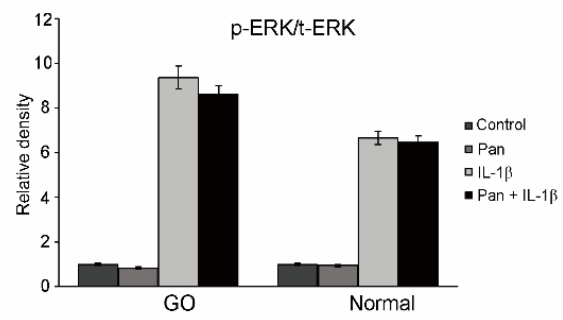
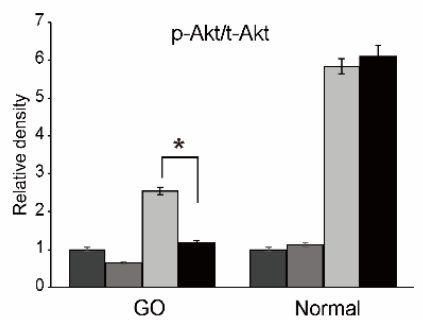
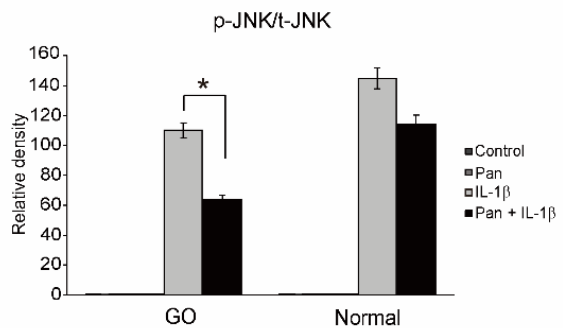
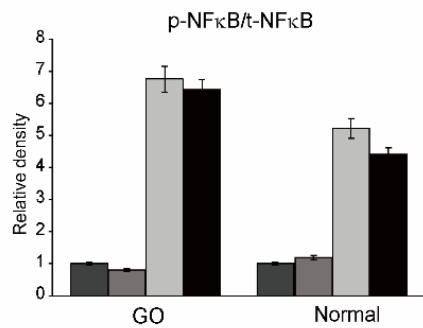
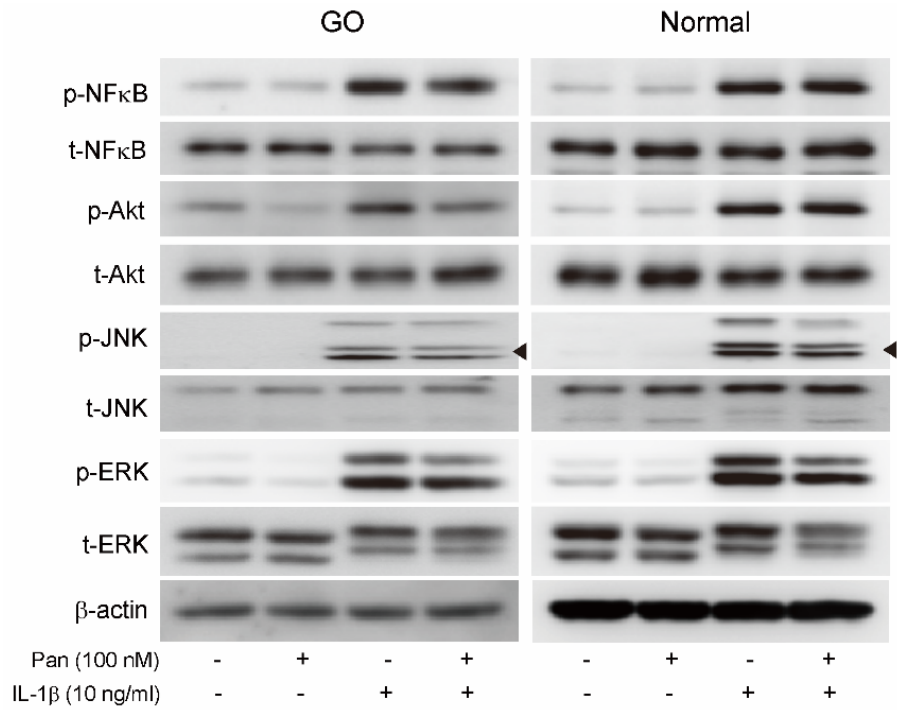
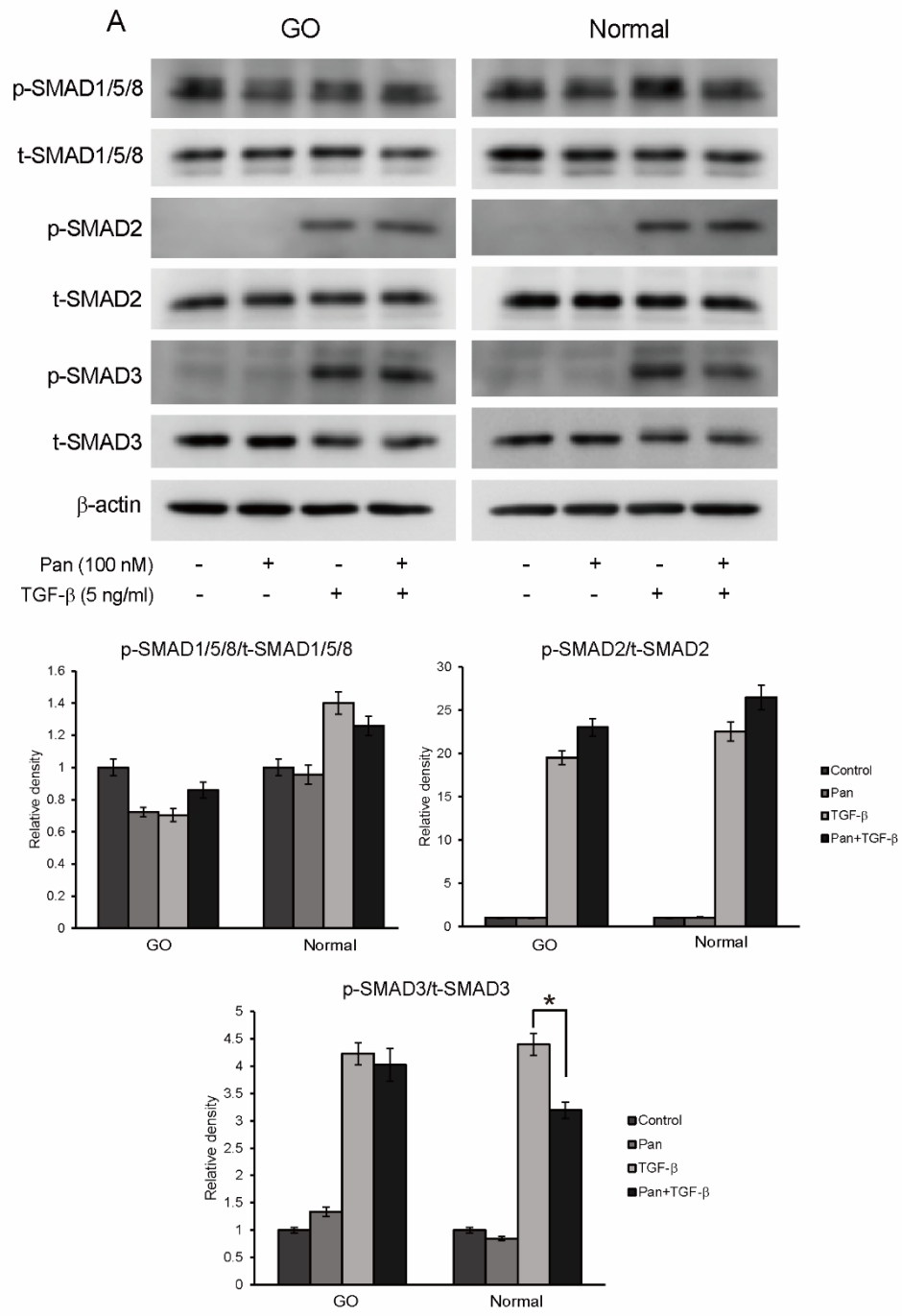


Figure 8. Effect of Panobinostat on signal proteins under IL-1 β stimulation. Orbital fibroblasts from GO (n=3) and normal (n=3) were pretreated with Panobinostat (100nM) for 24 hours, followed by IL-1 β (10ng/ml) for 15 minutes. Total (t-) and phosphorylated (p-) pathway molecules, NF- κ B, Akt, JNK, and ERK, were analyzed with western blotting. The representative western blot gel images are shown. β -actin was a loading control. After quantification using densitometry, the ratio of p- and t- pathway molecules were measured and relatively presented compared to the control. The results of the graphs are shown as relative mean density \pm SD (* p <0.05 versus without Panobinostat).

Upon TGF- β stimulation, SMAD and non-SMAD signaling are induced.²⁶ As a major transducer of TGF- β , SMAD pathway molecules, SMAD 1/5/8, SMAD 2, and SMAD 3, were investigated to find the effect of Panobinostat. Culture with 100nM Panobinostat for 3 hours significantly reduced TGF- β (5ng/ml, 1 hour) induced SMAD 3 phosphorylation more predominantly in normal cells (* p <0.05) (Figure 9A). As non-SMAD pathway molecules, Akt, JNK, p38, and ERK expressions were examined under TGF- β stimulation (5ng/ml, 1 hour) after Panobinostat (100nM) exposure for 3 hours. Phosphorylation of Akt was attenuated by treatment with Panobinostat in both GO and normal cells, and phosphorylation of p38 was reduced in normal cells (* p <0.05) (Figure 9B).



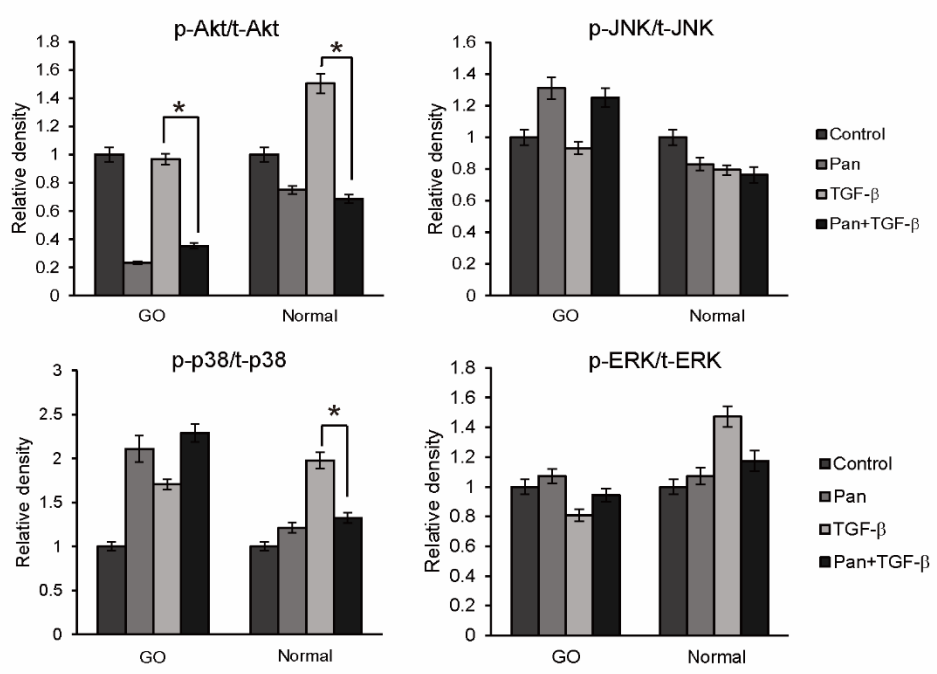
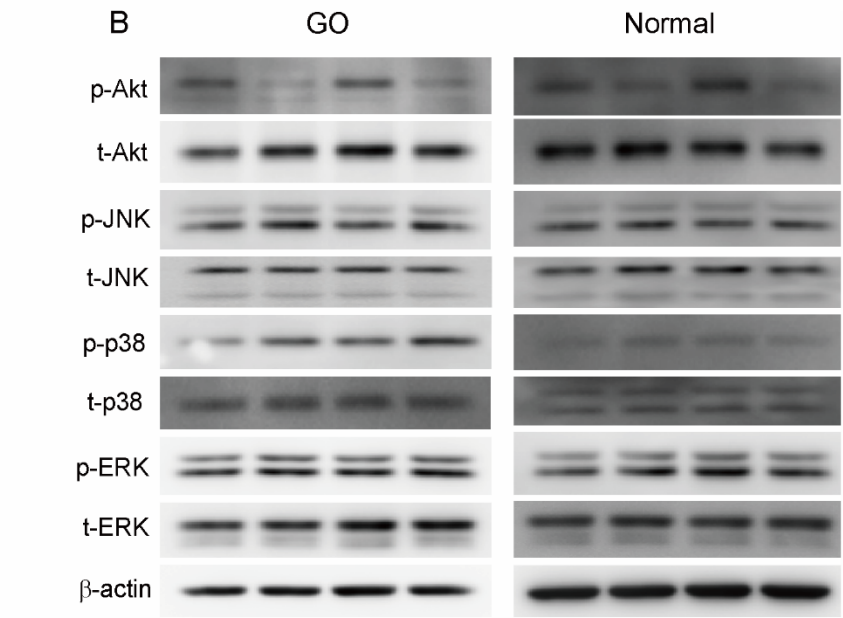


Figure 9. Effect of Panobinostat on signal proteins under TGF- β stimulation. (A) Orbital fibroblasts were exposed to 100nM of Panobinostat for 3 hours, and then stimulated with TGF- β (5 ng/ml) for 1 hour. Phosphorylated (p-) and total (t-) SMAD signaling transducers, SMAD1/5/8, SMAD2, and SMAD3, were analyzed by western blotting. (B) Non-SMAD pathways under TGF- β (5 ng/ml) stimulation for 1 hour were examined on orbital fibroblasts. 100nM of Panobinostat was pretreated for 3 hours before TGF- β treatment. Western blot analysis of p- and t- form of non-SMAD pathway molecules, Akt, JNK, p38, and ERK, was done. Orbital fibroblasts from three different GO and normal subjects were used. β -actin was a loading control. The ratio of p- form divided by t- form was relatively expressed by control, and mean density \pm SD was indicated (* p <0.05 versus without Panobinostat).

6. The role of HDAC7 in GO orbital fibroblasts

Based on the previous results that HDAC7 showed notable suppression by Panobinostat (Figure 4), the effects of HDAC7 on GO orbital fibroblasts were examined. GO orbital fibroblasts were treated with IL-1 β (10ng/ml) and TGF- β (5ng/ml) for different times, 0, 5, 10, 30, and 60 minutes. Western blot analysis revealed that HDAC7 protein level was increased after 30 minutes in response to the IL-1 β , and 60 minutes of TGF- β stimulation (* p <0.05) (Figure 10).

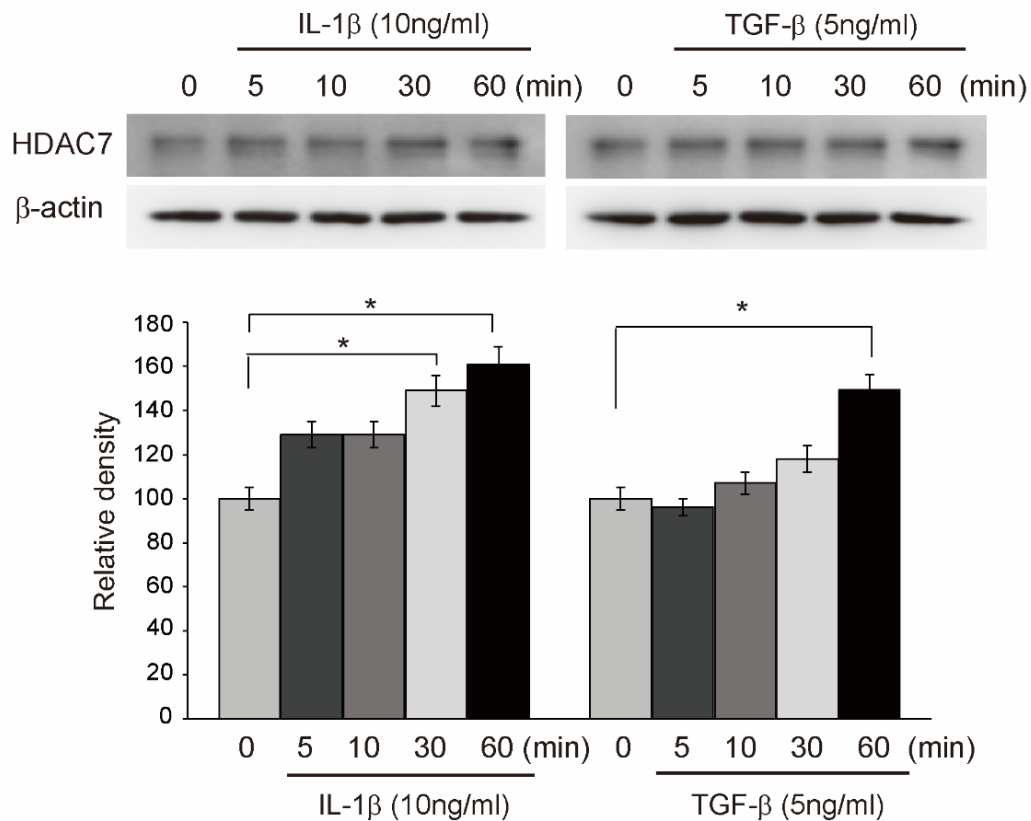


Figure 10. HDAC7 expression under stimulation of IL-1 β and TGF- β in GO orbital fibroblasts. Orbital fibroblasts from GO (n=3) were stimulated with IL-1 β (10 ng/ml) and TGF- β (5 ng/ml) over increasing time intervals (0-60 minutes). HDAC7 release was measured in the times indicated (0, 5, 10, 30, and 60 minutes) by western blot analysis. Representative western blot gel images were presented. β -actin was a loading control. Data measured with densitometry was represented as the mean \pm SD of duplicate experiments for three different individuals (*p < 0.05 versus cells without stimulation).

To clarify the role of HDAC7, HDAC7 siRNA silencing was conducted. siRNA for HDAC7 (si-HDAC7) and control siRNA (si-con) was transfected for 24 hours, and then stimulated with IL-1 β (10 ng/ml) or TGF- β (5 ng/ml) for 24 hours to evaluate the effect on inflammation or fibrosis. IL-6 which was increased following IL-1 β treatment was

significantly reduced in the orbital fibroblasts with the si-HDAC7 transfection ($*p < 0.05$) (Figure 11A). HDAC7 inhibition significantly reduced the TGF- β induced profibrotic proteins, fibronectin and α -SMA in both GO and normal orbital fibroblasts, and Col I α and Col 3 in GO cells ($*p < 0.05$) (Figure 11B).

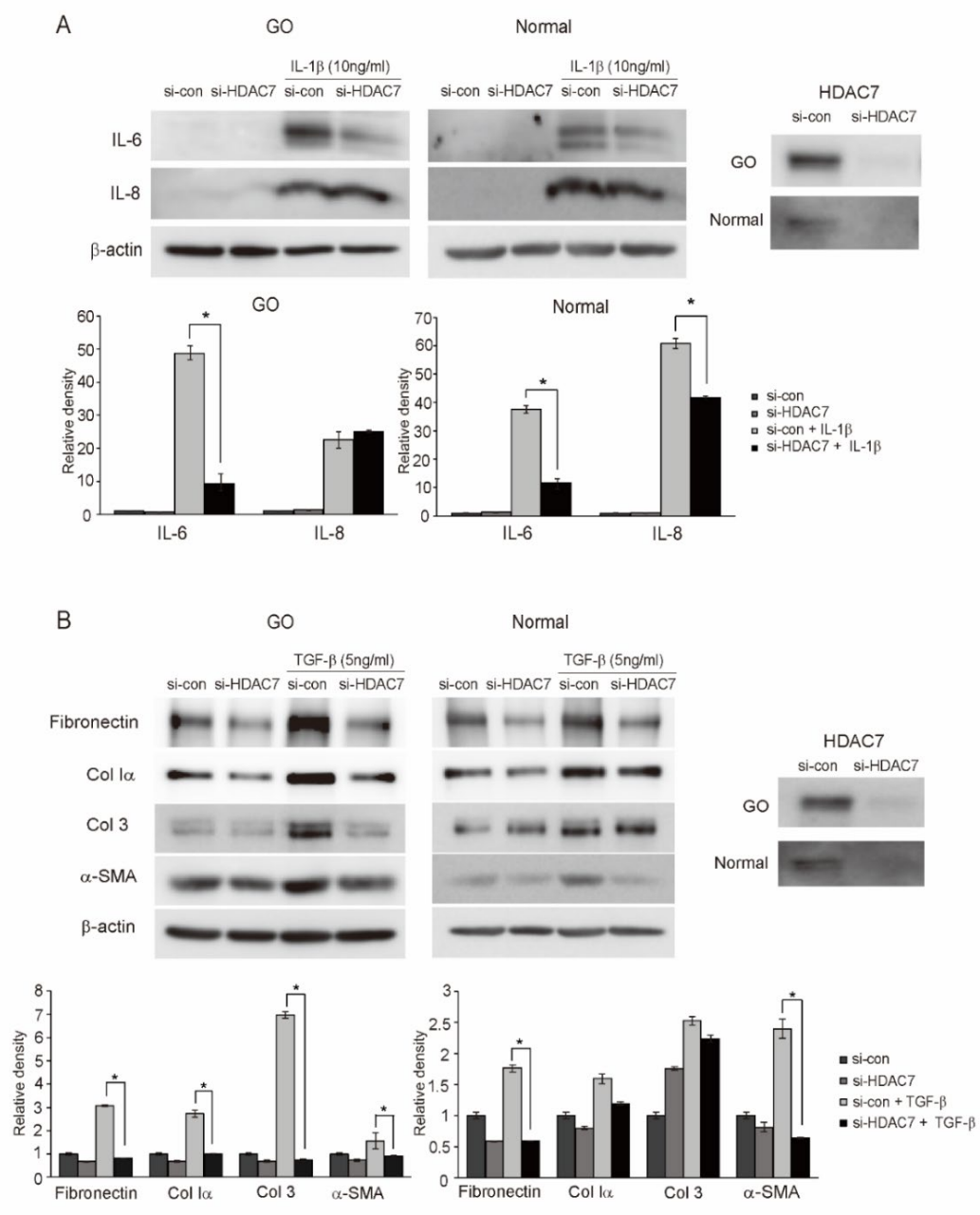


Figure 11. Anti-inflammatory and anti-fibrotic effects of silencing HDAC7 in orbital fibroblasts. *HDAC7* was knocked down by transfecting of siRNA (10nM) for 24 hours and maintaining for 48 hours. GO and normal orbital fibroblasts (n=3) showed the silencing

efficiency of si-HDAC7 as compared with si-con. (A) IL-1 β (10 ng/ml) stimulation proceeded for 24 hours. Western blot analyses were performed to investigate proinflammatory cytokines, IL-6 and IL-8. (B) TGF- β (5 ng/ml) was treated for 24 hours. Profibrotic proteins, fibronectin, collagen I α , collagen 3, and α -SMA, were measured using western blot analysis. β -actin was used as a loading control for normalization. Each experiment was performed twice. Bars represent values of relative density with the mean \pm SD (* p < 0.05).

Additional experiments were performed to determine the effects of HDAC3 and HDAC6 which showed significant changes to Panobinostat. In Figure 4., HDAC6 mRNA expression was suppressed by Panobinostat treatment. We knocked down *HDAC6* with siRNA transfection, and the orbital fibroblasts were treated with IL-1 β (10 ng/ml) or TGF- β (5 ng/ml). Protein levels of the IL-1 β -induced proinflammatory cytokines, IL-6 and IL-8, did not differ between cells with siRNA transfection for HDAC6 (si-HDAC6) and control (si-con) (Figure 12A). Upon TGF- β stimulation, profibrotic proteins, fibronectin and α -SMA, were down-regulated with si-HDAC6 transfection in normal cells, however, the other proteins, Col1 α and Col3, in normal cells and all profibrotic proteins in GO cells showed no difference in si-HDAC6 transfection (* p < 0.05) (Figure 12B).

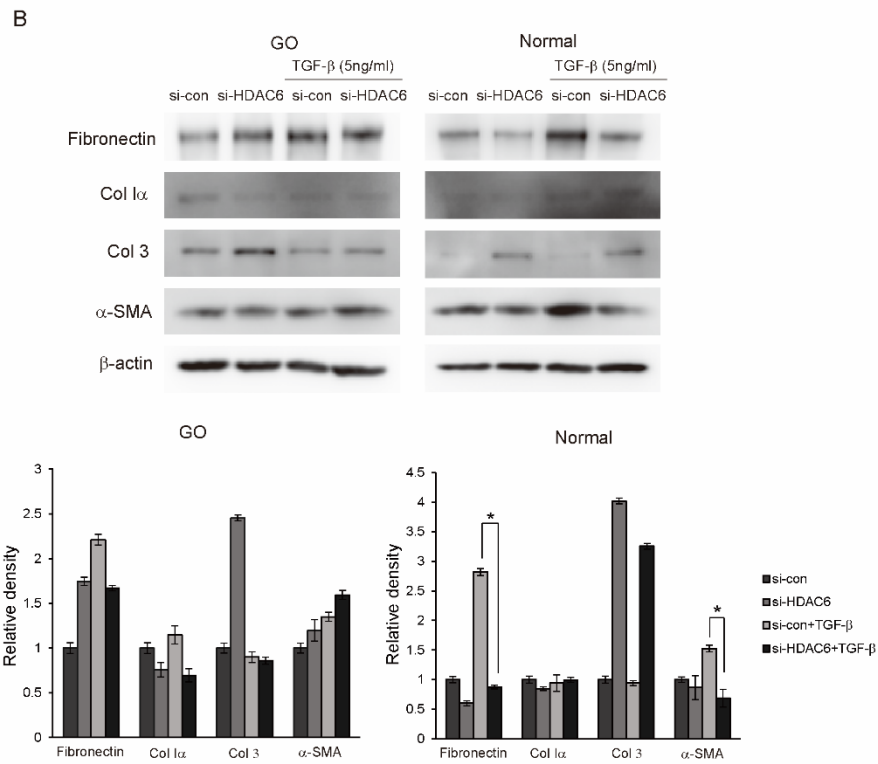
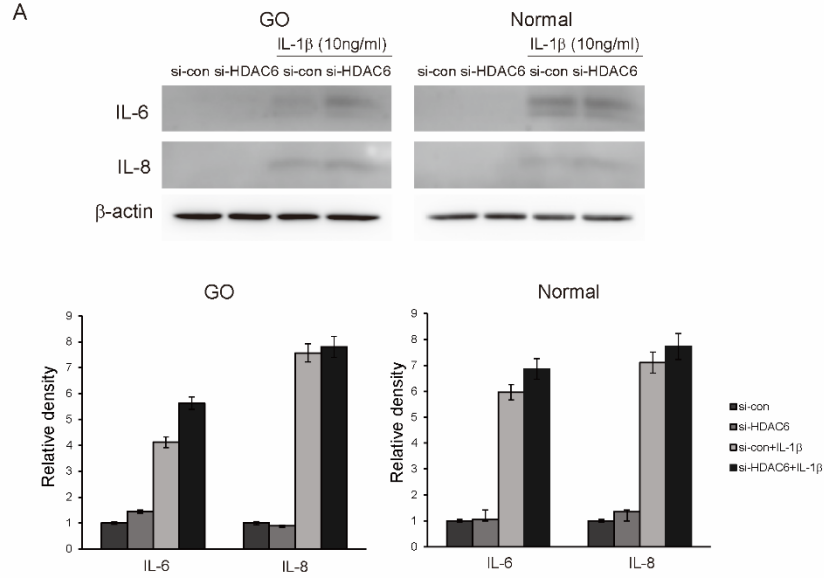


Figure 12. Effect of silencing HDAC6 on inflammation and fibrosis. Orbital fibroblasts from GO (n=3) and normal (n=3) subjects were transfected with si-HDAC6 (10ng) or si-con for 24 hours and maintained for 48 hours. (A) Following the treatment, orbital fibroblasts were stimulated with IL-1 β (10ng/ml) for 24 hours. Proinflammatory cytokines, IL-6 and IL-8, were analyzed with western blotting. (B) TGF- β (5ng/ml) was treated for 24 hours to the si-HDAC6 or si-con transfected cells. Profibrotic proteins, fibronectin, collagen I α , collagen 3, and α -SMA, were measured by western blot analysis. Values were normalized with β -actin and presented as relative to the control. Graphs are presented as the mean \pm SD from three independent experiments conducted twice.

In Figure 4, HDAC7 mRNA expression decreased, whereas HDAC3 mRNA expression was significantly upregulated by Panobinostat treatment. To determine whether HDAC7 inhibition directly affects anti-inflammation and anti-fibrosis not through the increased HDAC3, we investigated the effect of siHDAC7 on HDAC3 expression. The effect of Panobinostat on the expression of HDAC3 and HDAC7 in orbital fibroblasts was reconfirmed by the protein level using Western blotting, demonstrating down-regulation of HDAC7 and up-regulation of HDAC3 in accordance with the mRNA results (Figure 13). Silencing HDAC7 did not affect the protein expression of HDAC3 in orbital fibroblasts (Figure 13B). Therefore, it can be concluded that the anti-inflammatory and anti-fibrotic effects of Panobinostat are mediated by HDAC7 independently of HDAC3.

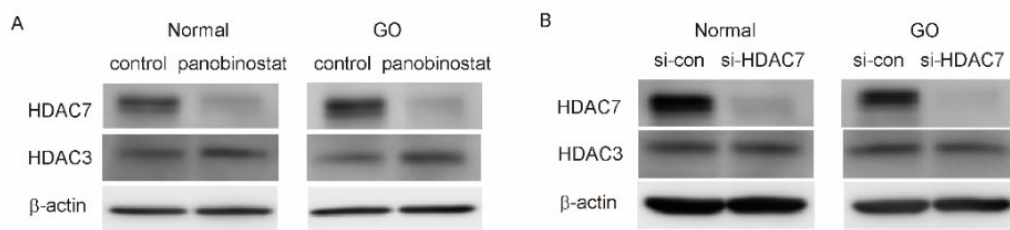


Figure 13. Expression of HDAC3 and HDAC7 in Panobinostat treatment and HDAC7 siRNA transfection. (A) Orbital fibroblasts were cultured with Panobinostat (100nM) for 24 hours. HDAC3 and HDAC7 protein expression levels were determined using western blotting. (B) After 24 hours of siRNA transfection for silencing *HDAC7* and its negative control followed by 48 hours of maintenance, the protein level of HDAC3 and HDAC7 was measured by western blot. All experiments were conducted twice in orbital fibroblasts from three different individuals. Representative gel images are shown.

IV. DISCUSSION

In this study, we identified Panobinostat, a pan-HDAC inhibitor, as a potent attenuator of orbital fibroblast activation. Panobinostat repressed the expression of pro-inflammatory, pro-fibrotic, and adipogenic proteins induced by each stimulator in orbital fibroblasts. We also investigated the role of Panobinostat in GO pathologic molecular pathways. Furthermore, Panobinostat showed a selective inhibitory effect on different HDACs in GO orbital fibroblasts, and especially blockage of HDAC7 had an association with the therapeutic effect of Panobinostat on GO pathogenesis.

Previous studies have investigated the association between HDACs and thyroid autoimmune disease. One study analyzed RNA levels of histone modifier genes such as HATs and HDACs isolated from PBMC, and HDAC1 and HDAC2 mRNA expressions were upregulated in PBMCs from GD patients, which induced histone H4 hypoacetylation.²⁷ Interestingly, our analysis found no differences in HDAC mRNA levels in PBMC between GO and normal individuals (Figure 2). The subjects of the previous study were composed of patients who were primarily diagnosed with GD without medication, whereas the GD duration of our patients was a mean of 5.5 years, and thyroid hormone levels were stable under medication (Table 2). Long-standing GD could manifest different aspects of HDAC expression, and it is feasible to deduce that the upregulation of HDAC is associated with the uncontrolled stage of GD. Similarly, this could also be applied to orbital tissue samples. Our tissue samples were mainly obtained as a byproduct from orbital decompression surgeries, usually undergone when the patient was in inactive stable GO. Most of the HDACs from GO orbital tissues showed lower mRNA expression levels than normal orbital tissues, possibly because of the negative feedback after the active phase (Figure 1). When IL-1 β and TGF- β were added to make an active stimulatory environment, HDAC7 protein expression was elevated (Figure 10). Other studies investigated the role of HDACs in GD and Hashimoto's thyroiditis (HT) in regards to class III HDAC and HDAC9, which we did not cover in this study.^{28,29} By demonstrating elevated HDAC9 expression in thyroid tissues and PBMC, particularly in T regulatory (Treg) lymphocytes, Sacristan-

Gomez et al. suggested that elevated HDAC9 in Tregs inhibits Treg activation, leading to the expansion of effector T cells and the production of inflammatory cytokines.²⁸ Yin et al. reported class III HDAC, Sirtuin1, expression is reduced in thyroid gland tissue and PBMC of patients with GD, allowing NF- κ B pathway activation.²⁹ When evaluating the in vivo application of pan-HDACi, it is important to consider the resulting impact on thyroid glands, mononuclear cells, as well as fibroblasts in relation to GD.

According to a recently published report about GO and HDAC, the expression of HDAC4 in orbital fibroblast of GO showed an upregulation in response to stimulation with platelet-derived growth factor-BB (PDGF-BB). HDAC4 silencing reduced Col1 α 1, α -SMA, Ki67, HAS2, and hyaluronic acid production induced by PDGF-BB stimulation.³⁰ These data suggested that acetylated lysine 9 of histone H3 potentially exacerbates the excessive production of extracellular matrix in GO fibroblasts. This is consistent with the current study linking that HDAC inhibition could be a potential therapy to alleviate the tissue remodeling of GO. Meanwhile, in contrast to previous study that primarily examined the production of hyaluronan, our research investigated proinflammatory cytokines, which are the more fundamental causes of GO, represented by IL-6 and IL-8. IL-6 enhances B-cell differentiation and antibody production, and stimulates TSHR expression in orbital fibroblasts, which amplifies inflammation.² Also, IL-6 may enhance adipogenesis in GO.³¹ IL-8 is also an important mediator as a chemoattractant and activator of neutrophils and lymphocytes.^{32,33} Moreover, we also focused on fibrosis, which leads to a restriction of eye movement and potentially results in long-lasting impairment. Lastly, PDGF-BB, which was used as a stimulator of orbital fibroblasts in the previous study, is a significant contributor to GO pathogenesis. Nevertheless, its source comes from immune cells stimulated by a plethora of cytokines such as IL-1 β , IFN- γ , TNF- α , and TGF- β .³⁴ Therefore, using more general regulators, including IL-1 β and TGF- β , as a stimulator and their blocking effects may have a more powerful impact on GO treatment.

The sensitivity of each HDAC inhibition by pan-HDACi varies in different cellular contexts, despite its pan-inhibitory nature.²⁵ For example, in myeloma cells, Vorinostat

exposure did not alter the expression of HDACs, however, Panobinostat upregulated most HDACs, especially HDAC6, and uniquely downregulated HDAC7.³⁵ In our study, Panobinostat showed selective inhibitory effect on the mRNA expression of individual HDACs in GO orbital fibroblasts, decreasing HDAC6, HDAC7, and increasing HDAC3 (Figure 4). In addition, HDAC7 suppression by Panobinostat was also verified in western blot analysis (Figure 7C, 7D). Similar to our findings, one of the other HDACi, trichostatin A (TSA) which has been known to inhibit class I and class II HDACs, exhibited an elevation of HDAC3 and a downregulation of HDAC7 in skin fibroblasts from systemic sclerosis patients.³⁶ To mitigate the adverse effects associated with Panobinostat, we aimed to explore the underlying mechanism of Panobinostat by selectively targeting specific HDACs. Specific inhibition using HDAC6 and HDAC7 siRNA clarified that the downregulation of HDAC7 is associated with the anti-inflammatory and anti-fibrotic effect of Panobinostat (Figure 11, 12). Meanwhile, since a previous study demonstrated that enzymatic activity of HDAC7 in the cell nucleus relies on HDAC3 binding mediated by SMRT and N-CoR,³⁷ we need to find out whether the therapeutic effect of Panobinostat is directly through HDAC7 reduction not mediated by elevated HDAC3. By verifying that HDAC7 reduction did not induce HDAC3 elevation, we could conclude that HDAC7 mediates the therapeutic effect of Panobinostat independently (Figure 13).

In orbital fibroblasts, TGF- β , a profibrotic cytokine, promotes the transformation of fibroblasts to myofibroblasts. Activated myofibroblasts express α -SMA which is critical for contractility and produce fibronectin and collagen. Particularly in the context of fibrosis, HDAC7 has been identified as a significant factor in the pathogenesis of inflammation-related diseases. Systemic sclerosis and Peyronie's disease are inflammatory diseases resulting in excessive fibrosis in the skin. Dr. Jungel's study group demonstrated cytokine-induced type I collagen and fibronectin were reduced upon treatment with TSA via inhibition of Smad transcription factors in systemic sclerosis skin fibroblasts.³⁸ They also showed diminished dermal accumulation of extracellular matrix in vivo mouse model. In the subsequent study, they analyzed the molecular mechanism of TSA-mediated antifibrosis

and verified that TGF- β induced type I and type III collagen was reduced by specific knockdown of HDAC7 in primary cultured systemic sclerosis fibroblasts.³⁶ In fibroblasts derived from Peyronie's plaque, HDAC7 silencing by HDAC7 siRNA limited the differentiation of fibroblasts into myofibroblasts and reduced the production of fibrotic extracellular matrix proteins such as collagen I, IV, and fibronectin.³⁹ In lung tissue from a mouse model of ovalbumin-induced airway fibrosis, protein expression of HDAC7 was increased.⁴⁰ Nuclear translocated HDAC7 in response to the stimulation of endothelin-1 (ET-1) promoted connective tissue growth factor (CTGF) production which has been implicated in fibroblast differentiation and systemic tissue fibrosis. In another study, as HDAC deacetylase lysins residues not only in histone proteins but also in non-histone proteins, HDAC7 was identified as a critical factor for HDAC-dependent deacetylation in the promoter region of anti-fibrotic gene PPARGC1A upon TGF- β stimulation.²⁰ HDAC could play an essential role in TGF- β mediated fibrosis activation by repressing the anti-fibrotic gene.

Several previous studies suggested HDAC inhibition may disrupt canonical TGF- β signaling, Smad-dependent pathway.^{38,39} In addition, it is not surprising that inhibition Akt phosphorylation alleviates GO inflammation and adipogenesis.^{41,42} However, our investigation on the downstream target of Panobinostat against proinflammatory and profibrotic stimulation in orbital fibroblasts suggested Akt is a possible signaling pathway molecule on either stimulation (Figure 8,9). In prior studies with IPF, prominent PI3k-Akt signaling pathways have been demonstrated. Tubastatin, a selective inhibitor of HDAC6, abrogated TGF- β induced type I collagen or cell proliferation by repressing Akt phosphorylation in lung fibroblast.^{43,44} Also, treatment of TSA blocked α -SMA expression in response to TGF- β , and it was dependent on HDAC4 mediated by phosphorylation of Akt.⁴⁵ Taken together, Akt signaling cascade contributes to the therapeutic impact of HDAC inhibition in regards to fibrosis as well as inflammation in GO.

Current clinical trials of HDACi are predominantly focused on cancer; however, with emerging reports, clinical trials for non-oncogenic diseases, including inflammatory

diseases, have also been investigated.⁴⁶ In order to reduce toxicity from pan-HDAC inhibition, an isoform-selective HDAC7 inhibitor is requested. Currently, only a limited number of potent HDAC7 inhibitors have been identified. These compounds exhibit high potency as inhibitors of HDAC7, but they also demonstrate inhibitory activity towards the other class IIa HDACs (HDAC4, 5, 9) to a comparable or lesser degree than HDAC7.⁴⁷ Class IIa HDACs exhibited high association with various immune cells, such as macrophages and lymphocytes.⁴⁸ Moreover, given that HDAC4 has been recognized as a target for hyaluronan production of GO,³⁰ it may be inferred that HDAC7 inhibitors have the potential to serve as a therapeutic intervention for GO even though they inhibit other class IIa HDACs. Further investigations are necessary when considering the application of HDAC7 inhibitors in an in vivo study.

In conclusion, Panobinostat could be a potential treatment option and HDAC7-specific inhibition could be a more effective therapy for GO. Our findings contribute to further understanding of GO pathogenesis and provide a crucial step toward the development of epigenetic-targeted treatments for GO. Further investigation on molecular mechanism and in-vivo study should be warranted.

V. CONCLUSION

Panobinostat, a pan-HDAC inhibitor, is a significant attenuator against pro-inflammatory, pro-adipogenic, and pro-fibrotic stimulations in primary cultured orbital fibroblasts from Graves' orbitopathy. Throughout the further investigation of the downstream molecular pathway, we demonstrated that Akt is associated with the anti-inflammatory and anti-fibrotic effect of Panobinostat. We confirmed a specific role of Panobinostat by analyzing mRNA expression of HDACs, and identified that HDAC7 is a key factor for the anti-inflammatory, anti-fibrosis effect of Panobinostat. In summary, our data indicates that Panobinostat exhibits promise as a potential treatment for GO. Furthermore, the specific inhibition of HDAC7 may contribute to advancing tailored therapeutics for GO by enhancing specificity and reducing toxicity.

REFERENCES

1. Lazarus JH. Epidemiology of Graves' orbitopathy (GO) and relationship with thyroid disease. *Best Pract Res Clin Endocrinol Metab.* Jun 2012;26(3):273-9.
2. Bahn RS. Graves' ophthalmopathy. *N Engl J Med.* Feb 25 2010;362(8):726-38.
3. Bartley GB, Fatourechhi V, Kadrmas EF, et al. Clinical features of Graves' ophthalmopathy in an incidence cohort. *Am J Ophthalmol.* Mar 1996;121(3):284-90.
4. Rotondo Dottore G, Torregrossa L, Lanzolla G, et al. Role of the mononuclear cell infiltrate in Graves' orbitopathy (GO): results of a large cohort study. *J Endocrinol Invest.* Mar 2022;45(3):563-572.
5. Huang Y, Fang S, Li D, Zhou H, Li B, Fan X. The involvement of T cell pathogenesis in thyroid-associated ophthalmopathy. *Eye (Lond).* Feb 2019;33(2):176-182.
6. Winn BJ, Kersten RC. Teprotumumab: Interpreting the Clinical Trials in the Context of Thyroid Eye Disease Pathogenesis and Current Therapies. *Ophthalmology.* Nov 2021;128(11):1627-1651.
7. Kossler AL, Douglas R, Dosiou C. Teprotumumab and the Evolving Therapeutic Landscape in Thyroid Eye Disease. *J Clin Endocrinol Metab.* Aug 8 2022;107(Suppl_1):S36-s46.
8. Yin X, Latif R, Bahn R, Davies TF. Genetic profiling in Graves' disease: further evidence for lack of a distinct genetic contribution to Graves' ophthalmopathy. *Thyroid.* Jul 2012;22(7):730-6.
9. Hadj-Kacem H, Rebuffat S, Mnif-Féki M, Belguith-Maalej S, Ayadi H, Péraldi-Roux S. Autoimmune thyroid diseases: genetic susceptibility of thyroid-specific genes and thyroid autoantigens contributions. *Int J Immunogenet.* Apr 2009;36(2):85-96.
10. Wang Y, Ma XM, Wang X, et al. Emerging Insights Into the Role of Epigenetics and Gut Microbiome in the Pathogenesis of Graves' Ophthalmopathy. *Front Endocrinol (Lausanne).* 2021;12:788535.
11. Kouzarides T. Chromatin modifications and their function. *Cell.* Feb 23

- 2007;128(4):693-705.
12. Shakespear MR, Halili MA, Irvine KM, Fairlie DP, Sweet MJ. Histone deacetylases as regulators of inflammation and immunity. *Trends Immunol.* Jul 2011;32(7):335-43.
 13. Narita T, Weinert BT, Choudhary C. Functions and mechanisms of non-histone protein acetylation. *Nat Rev Mol Cell Biol.* Mar 2019;20(3):156-174.
 14. Gatla HR, Muniraj N, Thevkar P, Yavvari S, Sukhavasi S, Makena MR. Regulation of Chemokines and Cytokines by Histone Deacetylases and an Update on Histone Decetylase Inhibitors in Human Diseases. *Int J Mol Sci.* Mar 5 2019;20(5).
 15. Smith TJ. Insights into the role of fibroblasts in human autoimmune diseases. *Clin Exp Immunol.* Sep 2005;141(3):388-97.
 16. Chen H, Pan J, Wang JD, Liao QM, Xia XR. Suberoylanilide Hydroxamic Acid, an Inhibitor of Histone Deacetylase, Induces Apoptosis in Rheumatoid Arthritis Fibroblast-Like Synoviocytes. *Inflammation.* Feb 2016;39(1):39-46.
 17. Zhang Y, Zhang B. Trichostatin A, an Inhibitor of Histone Deacetylase, Inhibits the Viability and Invasiveness of Hypoxic Rheumatoid Arthritis Fibroblast-Like Synoviocytes via PI3K/Akt Signaling. *J Biochem Mol Toxicol.* Apr 2016;30(4):163-9.
 18. Oh BR, Suh DH, Bae D, et al. Therapeutic effect of a novel histone deacetylase 6 inhibitor, CKD-L, on collagen-induced arthritis in vivo and regulatory T cells in rheumatoid arthritis in vitro. *Arthritis Res Ther.* Jul 3 2017;19(1):154.
 19. de Zoeten EF, Wang L, Butler K, et al. Histone deacetylase 6 and heat shock protein 90 control the functions of Foxp3(+) T-regulatory cells. *Mol Cell Biol.* May 2011;31(10):2066-78.
 20. Jones DL, Haak AJ, Caporarello N, et al. TGF β -induced fibroblast activation requires persistent and targeted HDAC-mediated gene repression. *J Cell Sci.* Oct 18 2019;132(20).
 21. Korfei M, Stelmaszek D, MacKenzie B, et al. Comparison of the antifibrotic effects of the pan-histone deacetylase-inhibitor panobinostat versus the IPF-drug

- pirfenidone in fibroblasts from patients with idiopathic pulmonary fibrosis. *PLoS One*. 2018;13(11):e0207915.
22. Sanders YY, Hagood JS, Liu H, Zhang W, Ambalavanan N, Thannickal VJ. Histone deacetylase inhibition promotes fibroblast apoptosis and ameliorates pulmonary fibrosis in mice. *Eur Respir J*. May 2014;43(5):1448-58.
 23. Atadja P. Development of the pan-DAC inhibitor panobinostat (LBH589): successes and challenges. *Cancer Lett*. Aug 8 2009;280(2):233-41.
 24. Shao W, Growney J, Feng Y, et al. Potent anticancer activity of a pan-deacetylase inhibitor panobinostat (LBH589) as a single agent in in vitro and in vivo tumor models. *Cancer Research*. 2008;68(9_Supplement):735-735.
 25. Dokmanovic M, Perez G, Xu W, et al. Histone deacetylase inhibitors selectively suppress expression of HDAC7. *Mol Cancer Ther*. Sep 2007;6(9):2525-34.
 26. Derynck R, Budi EH. Specificity, versatility, and control of TGF- β family signaling. *Sci Signal*. Feb 26 2019;12(570).
 27. Yan N, Zhou JZ, Zhang JA, et al. Histone hypoacetylation and increased histone deacetylases in peripheral blood mononuclear cells from patients with Graves' disease. *Mol Cell Endocrinol*. Oct 15 2015;414:143-7.
 28. Sacristán-Gómez P, Serrano-Somavilla A, González-Amaro R, Martínez-Hernández R, Marazuela M. Analysis of Expression of Different Histone Deacetylases in Autoimmune Thyroid Disease. *J Clin Endocrinol Metab*. Oct 21 2021;106(11):3213-3227.
 29. Yin Q, Shen L, Qi Y, et al. Decreased SIRT1 expression in the peripheral blood of patients with Graves' disease. *J Endocrinol*. Aug 2020;246(2):161-173.
 30. Ekronarongchai S, Palaga T, Saonanon P, et al. Histone Deacetylase 4 Controls Extracellular Matrix Production in Orbital Fibroblasts from Graves' Ophthalmopathy Patients. *Thyroid*. Oct 2021;31(10):1566-1576.
 31. Bahn RS. Thyrotropin receptor expression in orbital adipose/connective tissues from patients with thyroid-associated ophthalmopathy. *Thyroid*. Mar 2002;12(3):193-5.

32. Xie K. Interleukin-8 and human cancer biology. *Cytokine Growth Factor Rev.* Dec 2001;12(4):375-91.
33. Sampson AP. The role of eosinophils and neutrophils in inflammation. *Clin Exp Allergy.* Jun 2000;30 Suppl 1:22-7.
34. Virakul S, van Steensel L, Dalm VA, Paridaens D, van Hagen PM, Dik WA. Platelet-derived growth factor: a key factor in the pathogenesis of graves' ophthalmopathy and potential target for treatment. *Eur Thyroid J.* Dec 2014;3(4):217-26.
35. Cheng T, Kiser K, Grasse L, et al. Expression of histone deacetylase (HDAC) family members in bortezomib-refractory multiple myeloma and modulation by panobinostat. *Cancer Drug Resist.* 2021;4(4):888-902.
36. Hemmatazad H, Rodrigues HM, Maurer B, et al. Histone deacetylase 7, a potential target for the antifibrotic treatment of systemic sclerosis. *Arthritis Rheum.* May 2009;60(5):1519-29.
37. Fischle W, Dequiedt F, Fillion M, Hendzel MJ, Voelter W, Verdin E. Human HDAC7 histone deacetylase activity is associated with HDAC3 in vivo. *J Biol Chem.* Sep 21 2001;276(38):35826-35.
38. Huber LC, Distler JH, Moritz F, et al. Trichostatin A prevents the accumulation of extracellular matrix in a mouse model of bleomycin-induced skin fibrosis. *Arthritis Rheum.* Aug 2007;56(8):2755-64.
39. Kang DH, Yin GN, Choi MJ, et al. Silencing Histone Deacetylase 7 Alleviates Transforming Growth Factor- β 1-Induced Profibrotic Responses in Fibroblasts Derived from Peyronie's Plaque. *World J Mens Health.* May 2018;36(2):139-146.
40. Hua HS, Wen HC, Weng CM, Lee HS, Chen BC, Lin CH. Histone deacetylase 7 mediates endothelin-1-induced connective tissue growth factor expression in human lung fibroblasts through p300 and activator protein-1 activation. *J Biomed Sci.* May 19 2021;28(1):38.
41. Kumar S, Nadeem S, Stan MN, Coenen M, Bahn RS. A stimulatory TSH receptor antibody enhances adipogenesis via phosphoinositide 3-kinase activation in orbital

- preadipocytes from patients with Graves' ophthalmopathy. *J Mol Endocrinol*. Jun 2011;46(3):155-63.
42. Ko J, Kim JY, Lee EJ, Yoon JS. Inhibitory Effect of Idelalisib, a Selective Phosphatidylinositol 3-Kinase δ Inhibitor, on Adipogenesis in an In Vitro Model of Graves' Orbitopathy. *Invest Ophthalmol Vis Sci*. Sep 4 2018;59(11):4477-4485.
43. Saito S, Zhuang Y, Shan B, et al. Tubastatin ameliorates pulmonary fibrosis by targeting the TGF β -PI3K-Akt pathway. *PLoS One*. 2017;12(10):e0186615.
44. Liu Y, Wang R, Han H, Li L. Tubastatin A suppresses the proliferation of fibroblasts in epidural fibrosis through phosphatidylinositol-3-kinase/protein kinase B/mammalian target of rapamycin (PI3K/AKT/mTOR) signalling pathway. *J Pharm Pharmacol*. Mar 1 2022;rgab106.
45. Guo W, Shan B, Klingsberg RC, Qin X, Lasky JA. Abrogation of TGF-beta1-induced fibroblast-myofibroblast differentiation by histone deacetylase inhibition. *Am J Physiol Lung Cell Mol Physiol*. Nov 2009;297(5):L864-70.
46. Bondarev AD, Attwood MM, Jonsson J, Chubarev VN, Tarasov VV, Schiöth HB. Recent developments of HDAC inhibitors: Emerging indications and novel molecules. *Br J Clin Pharmacol*. Dec 2021;87(12):4577-4597.
47. Wang Y, Abrol R, Mak JYW, et al. Histone deacetylase 7: a signalling hub controlling development, inflammation, metabolism and disease. *Febs j*. Jun 2023;290(11):2805-2832.
48. Liu L, Dong L, Bourguet E, Fairlie DP. Targeting Class IIa HDACs: Insights from Phenotypes and Inhibitors. *Curr Med Chem*. 2021;28(42):8628-8672.

ABSTRACT(IN KOREAN)

갑상선 안병증 *in vitro* 모델에서 HDAC inhibition의 치료적 역할

<지도교수 윤진숙>

연세대학교 대학원 의학과

변형주

갑상선안병증은 갑상선항진증 환자에서 나타나는 안와염증으로, 활성화된 안와섬유모세포에 의해 유발된 염증이 섬유화 또는 지방분화로 이어지는 것이 특징이다. Histone deacetylase (HDAC)은 histone acetyltransferase (HAT)와 상반되는 역할을 하며 히스톤단백질 및 그 외의 단백질에 deacetylation을 하는 효소로, 자가면역질환이나 섬유증에 관여한다고 알려져 있다. 또한, HDAC 억제제는 최근 혈액암에 대한 사용이 승인되어 널리 사용되고 있다. 이에 따라 우리는 갑상선안병증에서 HDAC 억제제의 치료제로서의 잠재력을 평가하기 위해 일차배양한 안와섬유모세포에서 HDAC 억제에 의한 영향을 확인하였다.

먼저, 갑상선 안병증환자와 정상환자의 안와조직과 혈액에서 HDAC의 mRNA 발현수준을 확인하였고, 일차배양한 안와섬유모세포에서 HDAC 억제제인 Panobinostat의 영향을 확인하였다. 안와섬유모세포에서 IL-1 β 혹은 TGF- β 자극하에 Panobinostat를 처리하여 발현되는 염증성 사이토카인(cytokine)이나 섬유증 및 지방형성에 관련한 단백질을 웨스턴블랏(western blot)을 이용하여 분석하였다. mRNA는 정량적 실시간 PCR을 통해 측정하였고, Oil red O 염색을 통해 세포내의 지질축적량을 정량화 하였다. Panobinostat의 세포특이적인 HDAC 억제효과를 평가하기 위해 갑상선안병증환자에서 채취하여 일차배양된 안와섬유모세포에서 Panobinostat에 의한 HDAC mRNA 발현억제정도를 다양한 HDAC에서 확인하였고, small interfering RNA (siRNA)를 세포에 transfection하여 특정 HDAC을 억제함으로써 다시 한번 더 확인하였다.

그 결과, Panobinostat는 IL-6, IL-8 과 같은 IL-1 β 유발 염증성 사이토카인과

collagen 1 α , collagen 3, α -SMA 및 fibronectin과 같은 TGF- β 유발 섬유증관련 단백질의 생성을 감소시켰다. 또한 갑상선 안와섬유모세포의 지방분화를 억제하였다. Panobinostat는 GO의 안와섬유모세포에서 HDAC7 mRNA 발현을 크게 약화시켰으며, siRNA를 이용하여 HDAC7을 특정적으로 억제시에 항염증 및 항섬유화 효과를 나타냈다.

Panobinostat은 *in vitro* 갑상선 안병증 세포모델이 되는 일차배양 안와섬유모세포에서 HDAC7 유전자 발현을 억제함으로써 염증성 사이토카인과 섬유화 단백질 및 지방의 생성을 억제하였다. 이에 따라 HDAC7은 GO의 염증, 지방생성 및 섬유증 메커니즘을 억제하는 잠재적인 표적이 될 수 있겠다. 향후 임상연구를 통해 약물의 안전성과 유효성에 대한 평가가 필요할 것이다.

핵심되는 말 : 갑상선 안병증, 안와 섬유모세포, Histone deacetylase (HDAC), HDAC inhibitor, Panobinostat, HDAC7